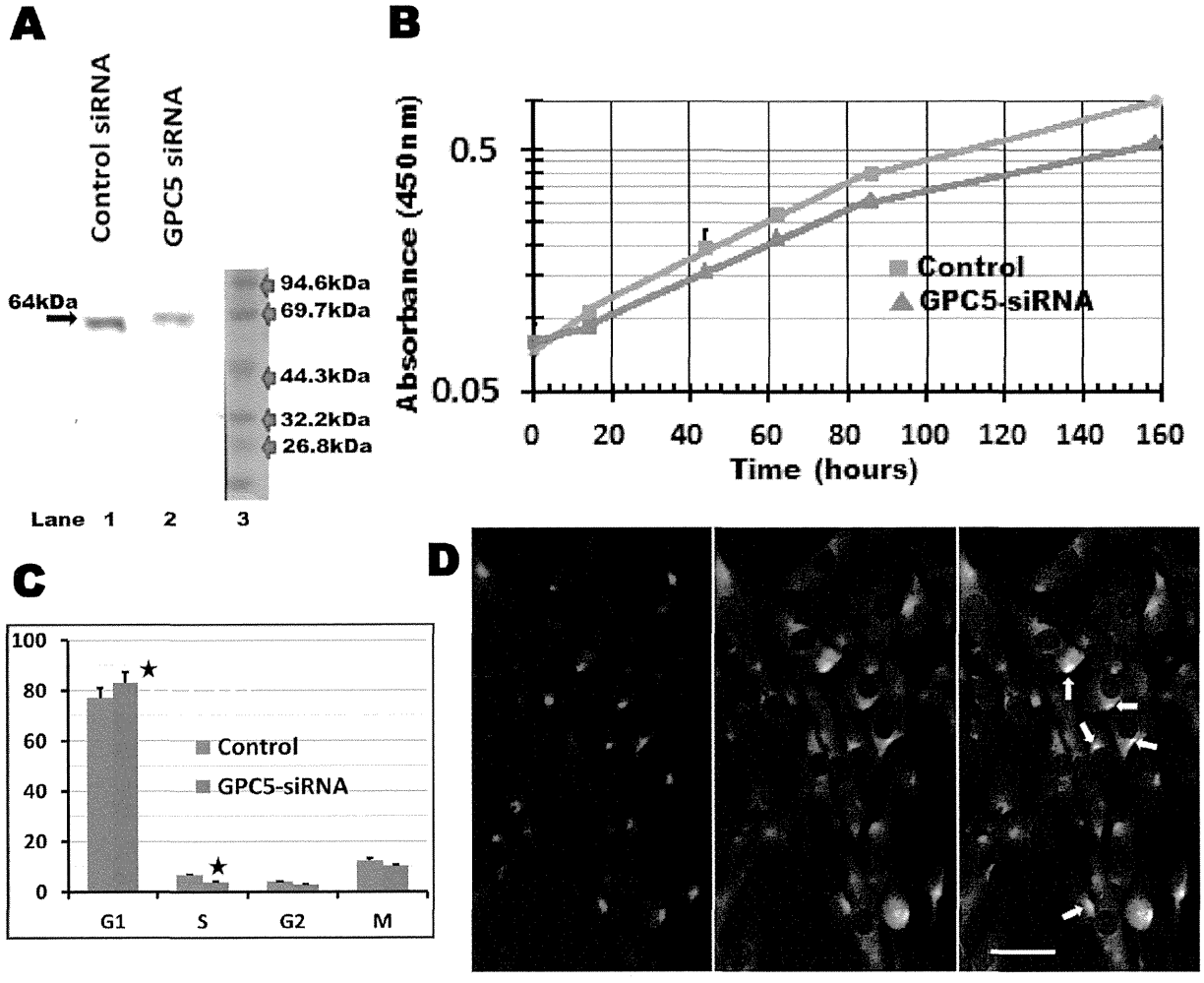

Fig 6. GPC5 expression affects proliferation in U3-DT cells. (**A**) Western blot analysis. Cells were treated with siRNA for 3 days. Cells were lysed and the levels of GPC5 were examined by Western blotting with anti-GPC5 Rabbit mAb. Lane 1, control siRNA-treated cells; Lane 2, GPC5 siRNA-treated cells; Lane 3, markers. (**B**) Growth curve. siRNA-treated cells (2,000 cells/well) were then seeded in 96-well culture plates and proliferation was assessed by CCK-8 assay at the indicated time points. An exponential approximation line of control (blue) or siRNA-treated (red) dots was drown between for 14 to 86hr. The results are expressed as the mean ± S.D. of quintuplicate wells. $P < 0.05$. (**C**) Cell-cycle distribution of U3-DT cells. Cell cycle distribution (%) of U3-DT cells incubated in medium containing siRNA (red) or not (blue) is shown. (**D**) Immunofluorescence profile of U3-DT cells. Double immunofluorescence labeling with anti-human GPC5 (red) and Ptc1 (green) antibodies in U3-DT cells. Nuclei are labeled with DAPI (merged image). Arrows: GPC5 and Ptc1 positive-merged spots (yellow) are clearly visible in U3-DT cells. Scale bar = 50 μm.

doi:10.1371/journal.pone.0126562.g006

provided several important pieces of evidence regarding transformation-related changes at different stages of prolonged culture. A summary of the alterations in cytological features and gene expression over the course of the transformation process is shown in Table 1.

First, we demonstrated that only mitotically defective near-triploid cells (U3-DT), present in a mixed cell population exhibiting chromosome instability (CIN), contributed to the tumorigenicity of UE6E7T-3 cells; however, tumors formed at 66% of injection sites, so, therefore, additional genetic alterations may be necessary for U3-DT cell tumorigenesis. The contribution of polyploidy cells to tumorigenesis has been demonstrated in other studies. Tetraploidy can promote CIN and tumorigenesis in p53-null mouse mammary epithelial cells [44] and in Pim-1-expressing human prostate and mammary epithelial cells [45]. U3-A cells with microsatellite

Table 1. Summary of cellular and genetic characteristics of UE6E7T-3 cells at four stages of transformation.

Stage	I	II	III	IV
PDL	60–90	91–150	151–230	231–295
Ploidy	diploid	aneuploid	mix polyploid	near-triploid
Number of chromosome (mode)	46	45	88	68
Cell shape	F	F	F	F
Doubling time (hr)	40	44	28	22
Growth in soft agar	negative	negative	slight	positive
Growth in mouse	NT	NT	NT	sarcoma
Oncogene	control	C	+++	+++
Tumor suppressor gene	control	+++	-	-
DNA repair gene (NHEJ)	control	+	+++	+++
CIN gene	control	++	+++	+++
Cell cycle activator	control	++	++	++
Cell cycle suppressor	control	+/-	-	-
Apoptosis activator	control	+++	-	-
Apoptosis inhibitor	control	C	++	+++
Growth factor, Signal transduction	control	+	+++	+++
Adhesion-related gene	control	++	-	-
Angiogenesis, Invasion, Metastasis	control	+/-	+/-	+/-

Note: (+), (-) and (C) denote the up-regulated, down-regulated, or control-level expression of major genes shown in Fig 3B. F, fibroblastic-like; NT, not tested.

doi:10.1371/journal.pone.0126562.t001

instability in chromosome 13 have a diploid karyotype during the first 90 PDL, and they preferentially lose one copy of chromosome 13 upon prolonged culture [22]. The loss of a whole chromosome 13, even a single copy, causes significant damage to near-diploid cells, but some survive (i.e., are selected), subsequently, acquire additional aneuploidy and tumor-related gene expression. Finally, unstable triploidy confers tumorigenicity and is a dominant feature of tumors. This karyotypic heterogeneity of genomes is consistent with the neoplastic progression theory [46], which holds that tumorigenesis occurs by a complex evolutionary process: according to this theory, progression develops as genetic instability is acquired, leading to the accumulation of genetic alterations and the continual selective outgrowth of variant subpopulations of tumor cells with a proliferative advantage.

By contrast, despite having a normal diploid karyotype with no detectable chromosome abnormalities, hTERT-transduced adult human MSCs (hTERT20) formed tumors after long-term culture [47]; however, these cells exhibit deletion of the Ink4a/ARF locus and epigenetic silencing of DBCCR1. A similar phenomenon was reported in hTERT-immortalized human fibroblast cell lines (WI-38, Leiden), which have a diploid karyotype and in which Ink4a is deleted [48,49]; however, these cell lines require active H-Ras or H-Ras and inactive p53 for tumor formation, resulting in the acquirement of chromosome abnormalities. Therefore, these reports suggest that h-TERT-mediated immortalization does not significantly affect genome integrity at the chromosome level, and that h-TERT-associated genetic and/or epigenetic alterations contribute to tumorigenicity rather than karyotype alterations. In addition, the genetic and/or epigenetic alterations may largely reflect differences in the pre-existing genetic makeup of each strain and the culture conditions.

Secondly, we showed that UE6E7T-3 acquired properties of transformed cells even without *RAS*- and *MYC*-mediated transduction. However, this transformation had a long latency,

requiring continuous *in vitro* passages. Significant overexpression of *RAS* was not detected at any stage of prolonged culture, suggesting that, at least for UE6E7T-3, the RAS pathway is not critical in transformation. This result is consistent with those of two previous studies [18,50], in contrast to other reports that RAS activation is an essential requirement for transformation [2–10]. We did, however, observe the marked up-regulation of other oncogenes (*BMI1*, *STAC*, *MYC*, *PIK3CA*, *RRAS2*, and *ATAD2*) in Stages III and IV. From these results, we infer that alternative pathways or currently unidentified factors may exist, which influence transformation in long-term culture.

Thirdly, we clearly demonstrated that numerous alterations in gene expression, in multiple pathways related to the acquisition of increased tumorigenicity, occurred spontaneously over prolonged culture. Our analysis of gene expression identified a crucial stage (Stage III), involving drastic changes in multiple pathways that determines the fate of UE6E7T-3 (Table 1). These changes included high expression of oncogenes as well as genes related to DNA-damage repair, chromosome instability, cell-cycle activation, inhibition of apoptosis, and increase of growth factors, concomitant with a strong depression of genes involved in tumor suppression, apoptosis, and adhesion. In particular, the suddenly increased expression of *MYC*, *BMI1*, *GPC5*, and *CIZ1* at this stage suggests that these genes play a key role in converting UE6E7T-3 to a tumorigenic state. *BMI1* encodes a key regulator in several cellular processes, including normal stem cell renewal and cancer cell proliferation [51]. The high expression of *BMI1* in U3-C and U3-DT suggests that these cells are tumorigenic. The main target of BMI1 is the *INK4A* locus, which encodes two structurally distinct proteins, $p16^{INK4a}$ and $p14^{ARF}$, both of which play important roles in cell-cycle regulation. In UE6E7T-3, up-regulation of *BMI1* could result in low *CDKN2A* ($p16^{INK4a}$-encoding gene) expression, allowing increased transcription of *E2F*, which would in turn lead to increased proliferation. *ATAD2* and *CIZ1*, which were also expressed at high levels in the late stages, are also highly expressed in a significant proportion of human tumors [38,52], suggesting that these genes contribute to proliferation, ultimately leading to transformation. Similar patterns were observed for apoptosis inhibitors and apoptosis accelerators (Fig 3Bf, and S2 and S3 Tables). When DNA damage is too extensive, checkpoint pathways trigger apoptosis. However, Stage III cells (U3-C) exhibited decreased expression of apoptosis-inducing genes and increased expression of anti-apoptotic genes. These cells failed to undergo apoptosis; the resulting spontaneous survivors (U3-DT) are distinct from U3-A and U3-B. Mutations arising from unrepaired DNA damage in normal human cells are prevented by the p53 and pRB checkpoint pathways, resulting in DNA repair, apoptosis, or senescence. Normal cells stop dividing until they have completed repair to their DNA. By contrast, genetically unstable UE6E7T-3 cells with defective DNA can easily avoid checkpoints due to breaks in their checkpoint pathways, and thereby maintain a higher rate of proliferation than normal cells. Such cells induce subsequent mutations by repetitive mitosis, over the course of which missegregation of whole chromosomes generates additional aneuploidy.

Similarly, expression of E-cadherin, a known tumor suppressor in many cancers [53,54], rapidly dropped at Stage III (Fig 3Bj, and S2 and S3 Tables). This shutdown was concomitant with the repression of expression of other adhesion genes, resulting in reduced cell-cell or cell-extracellular matrix interactions, suggestive of an invasive tendency. However, MMPs, which help to degrade extracellular matrix proteins, were expressed at lower levels in U3-C and U3-DT (Fig 3Bl, and S2 and S3 Tables). In addition, VEGFC, which along with MMPs is a major contributor to angiogenesis, was also expressed at low levels in U3-DT. VEGFC causes a signaling cascade resulting in maturation of endothelial cells into blood vessels. The low VEGFC expression suggests that cascade members downstream, including MMPs, VCAMs, and ICAMs, would not be stimulated, and U3-DT cells may be promoted with respect to

malignancy in future. Together, these alterations in gene expression in different core pathways strongly suggest that the transition of UE6E7T-3 into a tumorigenic state occurred at Stage III, concomitant with drastic alterations in chromosomal numbers and chromosomal structures. At the same time, expression of genes encoding tumor markers rose dramatically at this stage, and the cells acquired defects in their ability to differentiate into several lineages.

Finally, from this comprehensive genetic analyses, we identified molecular signatures in U3-DT that are commonly expressed in various types of tumors, as mentioned above, suggesting that transformants of many cell types show common signature in gene expression.

In addition, one important finding in this study pertains to the glypican-5-gene (GPC5)-related signaling. GPC5, which is a sarcoma cell marker [55], was markedly overexpressed at later culture stage in association with transformation of UE6E7T-3 cells. Other studies recently showed that GPC5 stimulates the proliferation of rhabdomyosarcoma (RMS) cells [28] and lung metastatic cells in salivary adenoid cystic carcinoma [56], while GPC5 may be a tumor suppressor in non-small cell lung cancer [57]. We have shown here that GPC5 augmented cell proliferation in UE6E7T-3 cell line (Fig 6). GPC5 encodes one of the six members of the glypican family (GPC1 to GPC6), heparan sulfate proteoglycans, which serve as essential modulators of key regulatory proteins such as Wnt, FGF, and Hh [58–60]. Li, et al. demonstrated that GPC5 acts as an activator of Hh signaling in RMS cell proliferation [28], whereas these authors have previously reported that GPC3 acts as an inhibitor of the same signaling in mouse embryo [61]. This indicates that two members of glypican family can display opposite roles in the regulation of Hh signaling. In UE6E7T-3 cell line, GPC3 is little expressed (S1 Table). In addition of marked overexpression of GPC5, a high level of expression of Hh signaling components (DHH, PTCH, and GLI1) was also found in U3-DT cells. Furthermore, DKK3, an inhibitor of the Wnt signaling, was overexpressed in U3-DT.

Based on these results, we propose that GPC5 stimulates the proliferation of U3-DT through the Hh signaling pathway by stabilizing the interaction between ligands and receptors. In human cerebellar granule cells, *BMI1* expression is up-regulated in response to sonic Hh protein (product of *SHH*) and parallels expression of *GLI1* [62]. *GLI1* overexpression induces *BMI1* expression, implying that *BMI1* is a downstream target in the Hh signaling pathway, and that its activation promotes cell proliferation by suppressing $p16^{INK4A}$. Therefore, *GPC5* may inhibit the Wnt signaling pathway and may also play an important role in the rapid proliferation of U3-DT at late stages, by regulating *BMI1* via the Hh signaling pathway. The possibility must be elucidated by future studies.

Expression of the *BCL11A*, *IL17REL*, and *CCDC3* genes was markedly elevated at Stage IV. Although BCL11A is an essential regulator of normal lymphocyte development in mouse embryos [63] and its expression is elevated in some lymphoma patients [64], the mechanism underlying this is unknown. The elevated expression of these genes suggests that they function in the tumorigenesis of U3-DT cells. In the future, we aim to clarify the functions of these genes in U3-DT cell tumorigenesis.

The results obtained in this study suggest that the UE6E7T-3 cell line can be used as a culture model for neoplastic transformation associated with dynamic alterations in gene expression and karyotype. Thus, this model may be a useful tool for assessing the functional contribution of genes showed by expression profiling to neoplastic transformation.

The cell lines generated in this study, each of which is characteristic of a particular stage in the transformation process, could have wider applications. U3-DT may prove useful for screening anticancer drugs, such as CtIP inhibitors, and U3-B might be useful for investigating the mechanisms of genetic aberration associated with neoplastic transformation or tumorigenesis. Furthermore, GPC5 might be a biomarker for sarcoma of human cells.

Supporting Information

S1 Method. Estimation of gene expression values by qRT-PCR. The qRT-PCR was performed by two methods.
(PDF)

S1 Fig. Cluster and pathway analyses of 8,032 genes expressed in U3-B,-C, and-DT. Cluster analysis of 8,032 genes performed using MeV software (**A**) and 'Diseases and Disorders' analysis using IPA software (**B**). The 'Diseases and Disorders' analysis revealed that 1,570 genes had expression patterns in U3-B, U3-C, and U3-DT that were characteristic of 'Cancer' (p-value, 1.92E-21), within which the 'Function' characteristics pinpointed 'Tumorigenesis' (**C**).
(TIF)

S2 Fig. Correlation between the qRT-PCR and the RNA-Seq data. (**A**) Relative expression values estimated by qRT-PCR or RNA-Seq. To validate the relative expression values generated by RNA-Seq, the relative expression values of 41 samples with 33 selected genes were calculated from qRT-PCR and RNA-Seq data. The correlation between two values was then verified statistically. (**B**) Correlation between the relative expression ratios calculated from the qRT-PCR and RNA-Seq data. The relative expression values of 41 samples calculated from qRT-PCR and RNA-Seq were plotted on the X-axis and Y-axis, respectively. Spearman's rank correlation coefficient, (R) was calculated in accordance with a formula described in Method B (S1 Method).
(TIF)

S1 Table. Gene expression value of 33,565 genes in U3-A, U3-B, U3-C, and U3-DT cells.
(PDF)

S2 Table. The relative expression value (REV) of 1,732 genes shown in Fig 3A. Expression value of U3-A,-B,-C, and-DT is the expression level of each gene divided by the level of GAPDH expression in the same sample. (*) Expression values for U3-A were obtained by dividing the value of each gene by that of GAPDH of U3-A, and then multiplying by 1,000. (**) REV of each gene in U3-A,-B,-C, and-DT is the expression level in U3-B,-C, or—DT divided by the expression level in U3-A.
(PDF)

S3 Table. List of genes shown in Fig 3B. Of the 1,732 genes listed in S1 Table, gene symbols and function of 180 genes (Fig 3B) are shown, in general, according to the NCBI gene database.
(PDF)

Acknowledgments

We thank Shin-ichi Tsunoda of the National Institutes of Biomedical Innovation, Health and Nutrition for encouraging this research, and Reiko Tanuma, Midori Ozawa and Akihiro Kohara for technical assistance during this study. We are grateful to Mahomi Suzuki (Molecular Devices Japan KK) for her assistance with ImageXpressMicro analysis. We also thank Keiko Uchida of the National Institutes of Biomedical Innovation, Health and Nutrition for skillful illustrations in the Figs.

Author Contributions

Conceived and designed the experiments: MT AH KT AU JT YK KA. Performed the experiments: KK-T JA TT. Analyzed the data: YH HM YM MK. Wrote the paper: MT AH KT.

References

1. Vogelstein B, Kinzler KW. Cancer genes and the pathways they control. Nat Med. 2004; 10: 789–799. PMID: 15286780
2. Hahn WC, Counter CM, Lundberg AS, Beijersbergen RL, Brooks MW, Weinberg RA. Creation of human tumour cells with defined genetic elements. Nature. 1999; 400: 464–468. PMID: 10440377
3. Akagi T, Sasai K, Hanafusa H. Refractory nature of normal human diploid fibroblasts with respect to oncogene-mediated transformation. Pros Natl Acad Sci U S A. 2003; 100: 13567–13572. PMID: 14597713
4. Drayton S, Rowe J, Jones R, Vatcheva R, Cuthbert-Heavens D, Marshall J, et al. Tumor suppressor $p16^{INK4a}$ determines sensitivity of human cells to transformation by cooperating cellular oncogenes. Cancer Cell. 2003; 4: 301–310. PMID: 14585357
5. Boehm JS, Hession MT, Bulmer SE, Hahn WC. Transformation of human and murine fibroblasts without viral oncoproteins. Mol Cell Biol. 2005; 25: 6464–6474. PMID: 16024784
6. Kendall SD, Linardic CM, Adam SJ, Counter CM. A Network of genetic events sufficient to convert normal human cells to a tumorigenic state. Cancer Res. 2005; 65: 9824–9828. PMID: 16267004
7. Funes JM, Quintero M, Henderson S, Martinez D, Qureshi U, Westwood C, et al. Transformation of human mesenchymal stem cells increases their dependency on oxidative phosphorylation for energy production. Proc Natl Acad Sci U S A. 2007; 104: 6223–6228. PMID: 17384149
8. Mahale AM, Khan ZA, Igarashi M, Nanjangud GJ, Qiao RF, Yao S, et al. Clonal selection in malignant transformation of human fibroblasts transduced with defined cellular oncogenes. Cancer Res. 2008; 68: 1417–1426. doi: 10.1158/0008-5472.CAN-07-3021 PMID: 18316605
9. Narisawa-Saito M, Yoshimatsu Y, Ohno S, Yugawa T, Egawa N, Fujita M, et al. An in vitro multistep carcinogenesis model for human cervical cancer. Cancer Res. 2008; 68: 5699–5705. doi: 10.1158/0008-5472.CAN-07-6862 PMID: 18632622
10. Sasai K, Sukezane T, Yanagida E, Nakagawa H, Hotta A, Itoh T, et al. Oncogene-mediated human lung epithelial cell transformation produces adenocarcinoma phenotypes in vivo. Cancer Res. 2011; 71: 2541–2549. doi: 10.1158/0008-5472.CAN-10-2221 PMID: 21447735
11. Li R, Sonik A, Stindl R, Rasnick D, Duesberg P. Aneuploidy vs. gene mutation hypothesis of cancer: Recent study claims mutation but is found to support aneuploidy. Proc Natl Acad Sci U S A. 2000; 97: 3236–3241. PMID: 10725343
12. Weaver BA, Silk AD, Montagna C, Verdier-Pinard P, Cleveland DW. Aneuploidy acts both oncogenically and as a tumor suppressor. Cancer Cell. 2007; 11: 25–36. PMID: 17189716
13. Baker DJ, Jeganathan KB, Cameron JD, Thompson M, Juneja S, Kopecka A, et al. BubR1 insufficiency causes early onset of aging-associated phenotypes and infertility in mice. Nat Genet. 2004; 36: 744–749. PMID: 15208629
14. Kalitsis P, Fowler KJ, Griffiths B, Earle E, Chow CW, Jamsen K, et al. Increased chromosome instability but not cancer predisposition in haploinsufficient Bub3 mice. Genes Chromosomes Cancer. 2005; 44: 29–36. PMID: 15898111
15. Jeganathan K, Malureanu L, Baker DJ, Abraham SC, van Deursen JM. Bub1 mediates cell death in response to chromosome missegregation and acts to suppress spontaneous tumorigenesis. J Cell Biol. 2007; 179: 255–267. PMID: 17938250
16. Torres EM, Williams BR, Tang YC, Amon A. Thoughts on aneuploidy. Cold Spring Harb Symp Quant Biol. 2010; 75: 445–451. doi: 10.1101/sqb.2010.75.025 PMID: 21289044
17. Burns JS, Abdallah BM, Guldberg P, Rygaard J, Schrøder HD, Kassem M. Tumorigenic heterogeneity in cancer stem cells evolved from long-term cultures of telomerase-immortalized human mesenchymal stem cells. Cancer Res. 2005; 65: 3126–3135. PMID: 15833842
18. Zongaro S, Stanchina E, Colombo T, D'Incalci M, Giulotto E, Mondello C, Stepwise neoplastic transformation of a telomerase immortalized fibroblast cell line. Cancer Res. 2005; 65: 11411–11418. PMID: 16357149
19. Milyavsky M, Tabach Y, Shats I, Erez N, Cohen Y, Tang X, et al. Transcriptional programs following genetic alterations *in p53*, *INK4A*, and *H-Ras* genes along defined stages of malignant transformation. Cancer Res. 2005; 65: 4530–4543. PMID: 15930270
20. Närvä E, Autio R, Rahkonen N, Kong L, Harrison N, Kitsberg D, et al. High-resolution DNA analysis of human embryonic stem cell lines reveals culture-induced copy number changes and loss of heterozygosity. Nat Biotechnol. 2010; 28: 371–377. doi: 10.1038/nbt.1615 PMID: 20351689
21. Takeuchi M, Takeuchi K, Kohara A, Satoh M, Shioda S, Ozawa Y, et al. Chromosomal instability in human mesenchymal stem cells immortalized with human papilloma virus E6, E7, and hTERT genes. In Vitro Cell Dev Biol Anim. 2007; 43: 129–138. PMID: 17514511

22. Takeuchi M, Takeuchi K, Ozawa Y, Kohara A, Mizusawa H. Aneuploidy in immortalized human mesenchymal stem cells with non-random loss of chromosome 13 in culture. In Vitro Cell Dev Biol Anim. 2009; 45: 290–299. doi: 10.1007/s11626-008-9174-1 PMID: 19184247

23. Imabayashi H, Mori T, Gojo S, Kiyono T, Sugiyama T, Irie R, et al. Redifferentiation of dedifferentiated chondrocytes and chondrogenesis of human bone marrow stromal cells via chondrosphere formation with expression profiling by large-scale cDNA analysis. Exp Cell Res. 2003; 288: 35–50. PMID: 12878157

24. Morton CL, Houghton PJ. Establishment of human tumor xenografts in immunodeficient mice. Nature Protocol. 2007; 2: 247–250. PMID: 17406581

25. Tuch BB, Laborde RR, Xu X, Gu J, Chung CB, Monighetti CK, et al. Tumor transcriptome sequencing reveals allelic expression imbalances associated with copy number alterations. PLoS ONE. 2010; 5(2): e9317. doi: 10.1371/journal.pone.0009317 PMID: 20174472

26. Higashino A, Sakate R, Kameoka Y, Takahashi I, Hirata M, Tanuma R, et al. Whole-genome sequencing and analysis of the Malaysian cynomolgus macaque (Macaca fascicularis) genome. Genome Biol. 2012; 13: R58. doi: 10.1186/gb-2012-13-7-r58 PMID: 22747675

27. Mortazavi A, Williams BA, McCue K, Schaeffer L, Wold B. Mapping and quantifying mammalian transcriptomes by RNA-Seq. Nat Methods. 2008; 5: 621–628. doi: 10.1038/nmeth.1226 PMID: 18516045

28. Li F, Shi W, Capurro M, Filmus J. Glypican-5 stimulates rhabdomyosarcoma cell proliferation by activating Hedgehog signaling. J Cell Biol. 2011; 192: 691–704. doi: 10.1083/jcb.201008087 PMID: 21339334

29. Kume H, Muraoka S, Kuga T, Adachi J, Narumi R, Watanabe S. et al. Discovery of colorectal cancer biomarker candidates by membrane proteomic analysis and subsequent verification using selected reaction monitoring (SRM) and tissue microarray (TMA) analysis. Mol Cell Proteomics. 2014; 13: 1471–1484. doi: 10.1074/mcp.M113.037093 PMID: 24687888

30. Nishiyama H, Gill JH, Pitt E, Kennedy W, Knowles MA. Negative regulation of G1/S transition by the candidate bladder tumour suppressor gene DBCCR1. Oncogene. 2001; 20: 2956–2964. PMID: 11420708

31. Serakinci N, Guldberg P, Burns JS, Abdallah B, Schrødder H, Jensen T, et al. Adult human mesenchymal stem cell as a target for neoplastic transformation. Oncogene. 2004; 23: 5095–5098. PMID: 15107831

32. Zou H, McGarry TJ, Bernal T, Kirschner MW. Identification of a vertebrate sister-chromatid separation inhibitor involved in transformation and tumorigenesis. Science. 1999; 285: 418–422. PMID: 10411507

33. Hernando E, Nahlé Z, Juan G, Diaz-Rodriguez E, Alaminos M, Hemann M, et al. Rb inactivation promotes genomic instability by uncoupling cell cycle progression from mitotic control. Nature. 2004; 430: 797–802. PMID: 15306814

34. Schvartzman JM, Duijf PH, Sotillo R, Coker C, Benezra R. Mad2 is a critical mediator of the chromosome instability observed upon Rb and p53 pathway inhibition. Cancer Cell. 2011; 19: 701–714. doi: 10.1016/j.ccr.2011.04.017 PMID: 21665145

35. Carter SL, Eklund AC, Kohane IS, Harris LN, Szallasi Z. A signature of chromosomal instability inferred from gene expression profiles predicts clinical outcome in multiple human cancers. Nat Genet. 2006; 38: 1043–1048. PMID: 16921376

36. Israels ED, Israels LG. The cell cycle. Oncologist. 2000; 5: 510–513. PMID: 11110604

37. Lukasik A, Uniewicz KA, Kulis M, Kozlowski P. Ciz1, a p21 $^{cip1/Waf1}$-interacting zinc finger protein and DNA replication factor, is a novel molecular partner for human enhancer of rudimentary homolog. FEBS J. 2008; 275: 332–340. PMID: 18081865

38. Ciró M, Prosperini E, Quarto M, Grazini U, Walfridsson J, McBlane F, et al. ATAD2 is a novel cofactor for MYC, overexpressed and amplified in aggressive tumors. Cancer Res. 2009; 69: 8491–8498. doi: 10.1158/0008-5472.CAN-09-2131 PMID: 19843847

39. Ryschich E, Huszty G, Knaebel HP, Hartel M, Büchler MW, Schmidt J. Transferrin receptor is a marker of malignant phenotype in human pancreatic cancer and in neuroendocrine carcinoma of the pancreas. Eur J Cancer. 2004; 40: 1418–1422. PMID: 15177502

40. Rohatgi R, Milenkovic L, Scott MP. Patched1 regulates hedgehog signaling at the primary cilium. Science. 2007; 317: 372–376. PMID: 17641202

41. Kiyono T, Foster SA, Koop JI, McDougall JK, Galloway DA, Klingelhutz AJ. Both Rb/p16^{INK4a} inactivation and telomerase activity are required to immortalize human epithelial cells. Nature. 1998; 396: 84–88. PMID: 9817205

42. Rodriguez R, Rubio R, Masip M, Catalina P, Nieto A, de la Cueva E, et al. Loss of p53 induces tumorigenesis in p21-deficient mesenchymal stem cells. Neoplasia. 2009; 11: 397–407. PMID: 19308294

43. Mohseny AB, Szuhai K, Romeo S, Buddingh EP, Briaire-de Bruijin I, de Jong D, et al. Osteosarcoma originates from mesenchymal stem cells in consequence of aneuploidization and genomic loss of Cdkn2. J Pathol. 2009; 219: 294–305. doi: 10.1002/path.2603 PMID: 19718709

44. Fujiwara T, Bandi M, Nitta M, Ivanova EV, Bronson RT, Pellman D. Cytokinesis failure generating tetraploids promotes tumorigenesis in p53-null cells. Nature. 2005; 437: 1043–1047. PMID: 16222300

45. Roh M, Franco OE, Hayward SW, van der Meer R, Abdulkadir SA. A role for polyploidy in the tumorigenicity of Pim-1-expressing human prostate and mammary epithelial cells. PLoS ONE. 2008; 3(7): e2572. doi: 10.1371/journal.pone.0002572 PMID: 18596907

46. Barrett MT, Sanchez CA, Prevo LJ, Wong DJ, Galipeau PC, Paulson TG, et al. Evolution of neoplastic cell lineages in Barrett oesophagus. Nat Genet. 1999; 22: 106–109. PMID: 10319873

47. Burns JS, Abdallah BM, Schrøder HD, Kassem M. The histopathology of a human mesenchymal stem cell experimental tumor model: support for an hMSC origin for Ewing's sarcoma?. Histol And Histopathol. 2008; 23: 1229–1240. PMID: 18712675

48. Milyavsky M, Shats I, Erez N, Tang X, Senderovich S, Meerson A, et al. Prolonged culture of telomerase-immortalized human fibroblasts leads to a premalignant phenotype. Cancer Res. 2003; 63: 7147–7157. PMID: 14612508

49. Brookes S, Rowe J, Ruas M, Llanos S, Clark PA, Lomax M, et al. INK4a-deficient human diploid fibroblasts are resistant to RAS-induced senescence. EMBO J. 2002; 21: 2936–2945. PMID: 12065407

50. Jin Y, Shima Y, Furu M, Aoyama T, Nakamata T, Nakayama T, et al. Absence of oncogenic mutations of RAS family genes in soft tissue sarcomas of 100 Japanese patients. Anticancer Res. 2010; 30: 245–252. PMID: 20150643

51. Leung C, Lingbeek M, Shakhova O, Liu J, Tanger E, Saremaslani P, et al. Bmi1 is essential for cerebellar development and is overexpressed in human medulloblastomas. Nature. 2004; 428: 337–341. PMID: 15029199

52. Rahman FA, Aziz N, Coverley D. Differential detection of alternatively spliced variants of Ciz1 in normal and cancer cells using a custom exon-junction microarray. BMC Cancer. 2010; 10: 482–493. doi: 10.1186/1471-2407-10-482 PMID: 20831784

53. Derksen PW, Liu X, Saridin F, van der Gulden H, Zevenhoven J, Evers B, et al. Somatic inactivation of E-cadherin and p53 in mice leads to metastatic lobular mammary carcinoma through induction of anoikis resistance and angiogenesis. Cancer Cell. 2006; 10: 437–449. PMID: 17097565

54. Derksen PW, Braumuller TM, van der Burg E, Hornsveld M, Mesman E, Wesseling J, et al. Mammary-specific inactivation of E-cadherin and p53 impairs functional gland development and leads to pleomorphic invasive lobular carcinoma in mice. Dis Model Mech. 2011; 4: 347–358. doi: 10.1242/dmm.006395 PMID: 21282721

55. Williamson D, Selfe J, Gordon T, Lu YJ, Pritchard-Jones K, Murai K, et al. Role for amplification and expression of glypican-5 in rhabdomyosarcoma. Cancer Res. 2007; 67: 57–65. PMID: 17210683

56. Zhang Y, Wang J, Dong F, Li H, Hou Y. The role of GPC5 in lung metastasis of salivary adenoid cystic carcinoma. Arch Oral Biol. 2014; 59: 1172–1182. doi: 10.1016/j.archoralbio.2014.07.009 PMID: 25093697

57. Yang X, Zhang Z, Qiu M, Hu J, Fan X, Wang J, et al. Glypican-5 is a novel metastasis suppressor gene in non-small cell lung cancer. Cancer Lett. 2013; 341: 265–273. doi: 10.1016/j.canlet.2013.08.020 PMID: 23962560

58. Filmus J, Capurro M, Rast J. Glypicans. Genome Biol. 2008; 9: 224.1–224.6. doi: 10.1186/gb-2008-9-5-224 PMID: 18505598

59. Li Y, Yang P. GPC5 gene and its related pathways in lung cancer. J Thorac Oncol. 2011; 6: 2–5. doi: 10.1097/JTO.0b013e3181fd6b04 PMID: 21178712

60. Filmus J, Capurro M. The role of glypicans in Hedgehog signaling. Matrix Biology. 2014; 35: 248–252. doi: 10.1016/j.matbio.2013.12.007 PMID: 24412155

61. Capurro MI, Xu P, Shi W, Li F, Jia A, Filmus J. Glypican-3 inhibits hedgehog signaling during development by competing with patched for hedgehog binding. Develop Cell. 2008; 14: 700–711.

62. Leung C, Lingbeek M, Shakhova O, Liu J, Tanger E, Saremaslani P, et al. Bmi1 is essential for cerebellar development and is overexpressed in human medulloblastomas. Nature. 2004; 428: 337–341. PMID: 15029199

63. Yu Y, Wang J, Khaled W, Burke S, Li P, Chen X, et al. Bcl11a is essential for lymphoid development and negatively regulates P53. J Exp Med. 2012; 209: 2467–2483. doi: 10.1084/jem.20121846 PMID: 23230003

64. Satterwhite E, Sonoki T, Willis TG, Harder L, Nowak R, Arriola EL, et al. The BCL11 gene family involvement of *BCL11A* in lymphoid malignancies. Blood. 2001; 98: 3413–3420. PMID: 11719382

Regenerative Therapy 1 (2015) 18–29

Contents lists available at ScienceDirect

Regenerative Therapy

journal homepage: http://www.elsevier.com/locate/reth

Original article

Xenogeneic-free defined conditions for derivation and expansion of human embryonic stem cells with mesenchymal stem cells

Hidenori Akutsu [a], Masakazu Machida [a], Seiichi Kanzaki [a], Tohru Sugawara [a], Takashi Ohkura [a], Naoko Nakamura [a], Mayu Yamazaki-Inoue [a], Takumi Miura [a], Mohan C. Vemuri [b], Mahendra S. Rao [c, 1], Kenji Miyado [a], Akihiro Umezawa [a, *]

[a] Department of Reproductive Biology, Center for Regenerative Medicine, National Research Institute for Child Health and Development, 2-10-1 Okura, Setagaya-ku, Tokyo 157-8535, Japan
[b] Thermo Fisher Scientific, 7335 Executive Way, Frederick, MD 21702, USA
[c] Center for Regenerative Medicine, National Institutes of Health, Bethesda, MD 20892, USA

ARTICLE INFO

Article history:
Received 20 July 2014
Received in revised form
17 December 2014
Accepted 28 December 2014

Keywords:
Human embryonic stem cells
Xenogeneic-free medium
Stem cell expansion
Human feeder layer
Mesenchymal stem cells
Gamma irradiation

ABSTRACT

The potential applications of human embryonic stem cells (hESCs) in regenerative medicine and developmental research have made stem cell biology one of the most fascinating and rapidly expanding fields of biomedicine. The first clinical trial of hESCs in humans has begun, and the field of stem cell therapy has just entered a new era. Here, we report seven hESC lines (SEES-1, -2, -3, -4, -5, -6, and -7). Four of them were derived and maintained on irradiated human mesenchymal stem cells (hMSCs) grown in xenogeneic-free defined media and substrate. Xenogeneic-free hMSCs isolated from the subcutaneous tissue of extra fingers from individuals with polydactyly showed appropriate potentials as feeder layers in the pluripotency and growth of hESCs. In this report, we describe a comprehensive characterization of these newly derived SEES cell lines. In addition, we developed a scalable culture system for hESCs having high biological safety by using gamma-irradiated serum replacement and pharmaceutical-grade recombinant basic fibroblast growth factor (bFGF, also known as trafermin). This is first report describing the maintenance of hESC pluripotency using pharmaceutical-grade human recombinant bFGF (trafermin) and gamma-irradiated serum replacement. Our defined medium system provides a path to scalability in Good Manufacturing Practice (GMP) settings for the generation of clinically relevant cell types from pluripotent cells for therapeutic applications.

© 2015, The Japanese Society for Regenerative Medicine. Production and hosting by Elsevier B.V. All rights reserved.

1. Introduction

Human pluripotent stem cells such as human embryonic stem cells (hESCs) and induced pluripotent stem cells (iPSCs) have remarkable developmental plasticity and therefore possess great potential for drug screening and the development of cellular models to study diseases. hESCs also have potential applications in regenerative medicine as source for cell-based therapy. Since the initial derivation of pluripotent hESCs by Thomson and colleagues in 1998 [1], more than 1000 hESC lines have been established and are now utilized in basic and clinical research worldwide [2]. Several clinical trials using hESC lines approved by the United States Food and Drug Administration (FDA) are currently underway. However, further research is still needed to facilitate the development of safer, reproducible, and scalable culture systems for the generation of hESCs for clinical and industrial purposes.

A key consideration with a cell therapy-compliant culture system, including safe expansion of hESCs, is the choice of culture media, matrix (including feeder layers), and passage procedures. Early hESC culture systems typically include the use of mouse embryonic fibroblast (MEF) feeders or medium conditioned on MEFs in the presence of serum or serum substitutes such as knockout serum replacement [1,3–6]. Human feeders and serum have also been used for hESC culture [7]; however, the use of serum or serum replacement, which contains undefined xenogeneic

* Corresponding author. Tel.: +81 3 5494 7047; fax: +81 3 5494 7048.
E-mail address: umezawa@1985.jukuin.keio.ac.jp (A. Umezawa).
Peer review under responsibility of the Japanese Society for Regenerative Medicine.
[1] Current affiliation: New York Stem Cell Foundation Research Institute, New York, NY 10032, USA.

http://dx.doi.org/10.1016/j.reth.2014.12.004
2352-3204/© 2015, The Japanese Society for Regenerative Medicine. Production and hosting by Elsevier B.V. All rights reserved.

factors, is still an issue for potential clinical applications of these cells. Transplantation of human cells exposed to animal-derived products can potentially transfer immunogenic sugars such as *N*-glycolylneuraminic acid (Neu5Gc) into the human body and may trigger chronic inflammation and immune reactions [8–10]. Recent studies have identified multiple factors that play a role in sustaining pluripotency and have led to the development of several defined medium systems for hESC culture and derivation [11–13]. Because no reports have described the successful establishment of hESCs in xenogeneic-free (XF) medium, it seems realistic to assume that the most reliable strategies for the establishment of clinical-grade hESCs include the use of a human feeder layer in XF medium, followed by expansion in a feeder-free culture system [14]. There are two strategies for developing hESC culture systems suitable for generation of clinically applicable cells. One approach is to establish XF, defined culture systems especially for future applications, and the other approach is to develop safe conditions for hESC culture systems while continuing to use xenogeneic products. In fact, ongoing clinical trials using hESCs employ conventional hESC culture systems, including mouse feeder layers, under certain conditions [15].

In this study, we developed a novel derivation/cultivation system of hESCs for potential application in translational and clinical research. To completely avoid exposure of hESCs to culture media with animal products, we established an XF culture system containing XF, defined culture medium with inactivated human mesenchymal stem cell (hMSC) feeders. The XF culture system with the hMSC feeder layers proved stable maintenance of self-renewal and pluripotency of newly established hESCs for more than 50 passages. Here, we report the successful derivation of four new hESC lines in this novel XF culture system. Furthermore, we evaluated replacement of a conventional hESC culture system with high-dose gamma-irradiated serum and pharmaceutical-grade recombinant basic fibroblast growth factor (bFGF) to provide insights into the development of a reproducible hESC cultivation system. We examined the pluripotency of SEES cell lines cultivated under the modified conventional culture system. hESCs were able to proliferate under the modified conventional conditions while retaining their pluripotency. Thus, our data provided clinically relevant alternative platforms for clinically and industrially applicable hESC culture systems.

2. Results

Since the first report describing the generation of hESCs by Thomson and coworkers [1], more than 1000 different hESC lines have been established worldwide [2]. Nevertheless, there is still a need for establishment of new hESC lines, particularly from certain HLA types and ethnic groups [16]. In this study, we derived seven new hESC lines using different culture conditions and developed a new hESC culture system using gamma-irradiated KO-SR and pharmaceutical-grade recombinant human bFGF (trafermin). Since our organization name is "Sei-iku" in Japanese, the hESC lines were designated as "SEES (Sei-iku embryonic stem)" in combination with numbers.

2.1. Stable derivation and culture of hESCs under serum replacement conditions

Out of five blastocysts, three hESC lines (SEES-1, SEES-2, and SEES-3) were derived from ICMs on MEF layers using the immunosurgery technique; conventional medium conditions, composed of HUES medium without human plasma protein fraction [4] (Fig. 1A), were used in this derivation. The pluripotency of each of these three SEES cell lines was confirmed by observation of typical morphology and positive immunostaining of stemness markers and differentiated derivatives comprising three embryonic germ layers (Supplemental Figs. 1 and 2). G-banding showed that SEES-1, SEES-2, and SEES-3 cells had normal karyotypes, i.e., 46,XX, 46,XX, and 46,XY, respectively (Supplemental Fig. 1).

2.2. Isolation and characterization of the XF hMSC feeder layer

Primary hMSCs isolated from subcutaneous tissue samples of juvenile donors undergoing surgical procedures for polydactyly were derived and expanded in a complete XF media system that contained an XF supplement, LipoMax, on a humanized substrate, CELLstart (Fig. 2A). Proliferation analysis was performed, and cell morphology was observed by light microscopy to confirm the proliferation assay results. Our data showed that cells grown in MSC-XF medium exhibited high proliferation rates and were self-renewing (Fig. 2B). Flow cytometric characterization was performed to compare surface marker expression characteristics of the

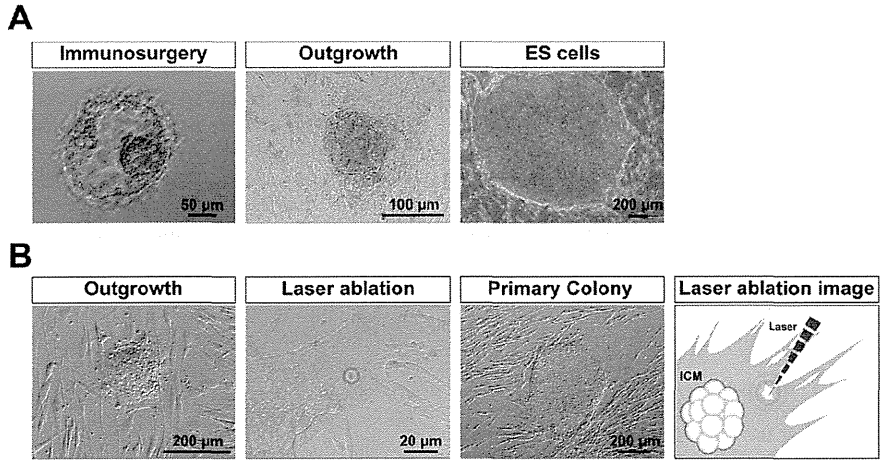

Fig. 1. Derivation of human ES cells by immunosurgery and laser ablation A) The intact inner cell mass (ICM) was isolated from blastocysts by immunosurgery. Cells of the trophectoderm are destroyed by brief exposure to antibodies directed against human cells in tandem with complement activity. Attachment and outgrowth of the ICM grew into an ESC (SEES-1) colony. B) The intact ICM was isolated by laser ablation without any animal products. Outgrowth of the blastocyst grown on human MSC feeder layers. Trophectoderm cells were targeted with multiple pulses of laser ablation. Typical morphology of ESC colonies was readily visible at high magnification. The image shows a schematic of ICM isolation by laser ablation, which is commonly used in artificial reproductive technology (ART).

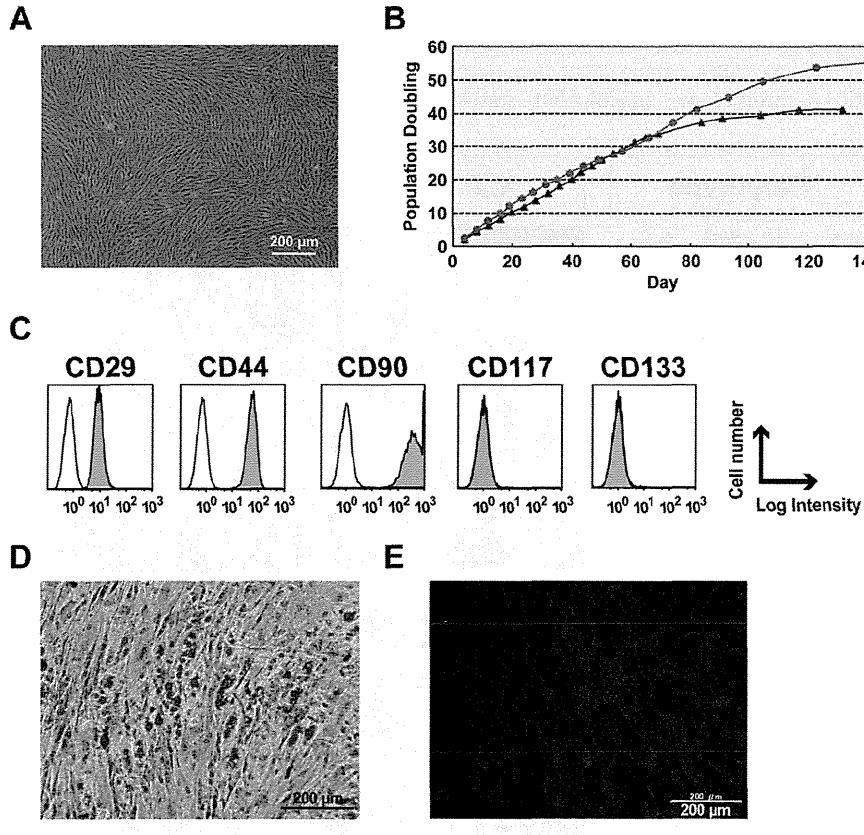

Fig. 2. Isolation and characterization of the xenogeneic-free hMSC feeder layer A) Primary human mesenchymal cells isolated from subcutaneous tissue of the polydactyly were expanded in xenogeneic-free media. B) Cells grew well over PD 30 under xenogeneic-free conditions. Two differentially isolated cell lines (red circle and blue triangle) showed similar cellular proliferation characteristics. C) Mesenchymal markers such as CD29, CD44, and CD90 were observed. D,E) The cells differentiated into adipogenic and osteogenic cells.

cells expanded in the MSC-XF medium. Positive CD29, CD44, and CD90 expression was observed, while CD117 and CD133 were not detected (Fig. 2C). Cells differentiated into both adipogenic and osteogenic cells (Fig. 2D and E). Taken together, our data demonstrated that cells isolated from polydactyly tissues could be classified as MSCs by flow cytometry analysis of their surface markers and evaluation of their multilineage differentiation potential.

2.3. Derivation of new hESC lines in XF culture conditions

To derive an XF hESC line, we first developed an XF culture system using XF hMSC feeder layers. We optimized an XF hESC medium composed of KO-DMEM supplemented with KO-SR XF, amino acids, vitamin C, bFGF, and two other growth factors (IGF1 and heregulin) [17]. All components of the medium were synthetic, recombinant, or of human origin. As a preliminary step, we confirmed the stable cultivation of SEES-1, SEES-2, and SEES-3 cells on XF hMSC feeder layers in XF hESC medium (data not shown). Twelve frozen human embryos were thawed and cultured to the blastocyst stage, and of these, eight blastocysts were used to derive XF hESC lines. Intact blastocysts, without immunosurgery, were plated onto irradiated XF hMSC layers in XF hESC medium. ICM isolation was carried out by exposing TE cells to cell-lethal laser pulses from an XYClone laser system (Fig. 1B). Finally, four XF hESC lines (SEES-4, SEES-5, SEES-6, and SEES-7) were generated and maintained stably (Fig. 3). All of these newly derived XF hESC lines were karyotyped regularly and exhibited a normal diploid karyotype, i.e., 46,XX, 46,XX, 46,XY, and 46,XX, respectively (Fig. 3). To assess the expression of a subset of stemness markers, these cell lines were analyzed by immunocytochemical staining; all XF SEES cell lines expressed the hESC markers NANOG, OCT3/4, SOX2, SSEA4, and TRA1-60 (Fig. 4). We also generated human iPSCs from XF Yub cells by over-expressing three reprogramming factors under hXF culture conditions using XF hESC medium and XF hMSC feeder layers. The XF human iPSCs were stably maintained and expressed the hESC markers such as OCT3/4, NANOG, SSEA4 and TRA1-60 (Supplemental Fig. 3).

2.4. hESCs cultured for prolonged periods in XF culture medium maintained their pluripotency and differentiation characteristics

To evaluate whether the newly derived XF SEES cell lines maintained their pluripotency *in vitro*, we performed EBs assays. EBs differentiated from the cells of SEES-4, SEES-5, SEES-6, and SEES-7 cells expressed markers associated with the three major germ layers: TUJ1 (ectoderm), αSMA (mesoderm), and AFP (endoderm; Fig. 5A). Additionally, in an *in vivo* pluripotency assay, structures from all three germ layers were detected, including neural tissues and pigmented epithelium (ectoderm), cartilage (mesoderm), and gut epithelial tissues (endoderm; Fig. 5B). Sialic acid was released from seven hESCs by acid hydrolysis and quantified by DMB-HPLC. Neu5Gc levels were increased in SEES-1, SEES-2, and SEES-3 cells, while the four XF SEES cell lines (SEES-4, SEES-5, SEES-6, and SEES-7) either did not express Neu5GC at all or had negligible levels of Neu5GC (Supplemental Fig. 4).

The seven SEES cell lines were further characterized by short tandem repeat (STR) analysis (Supplemental Table 1), HLA-DNA typing (Supplemental Table 2), ABO typing (Supplemental Fig. 5), and cytogenetic X-chromosome inactivation status analysis (Supplemental Fig. 6). The distinct features of SEES cell lines could be observed by STR and HLA profiling. SEES-2 and SEES-5 were blood type OO, which is most suitable for cellular transplantation.

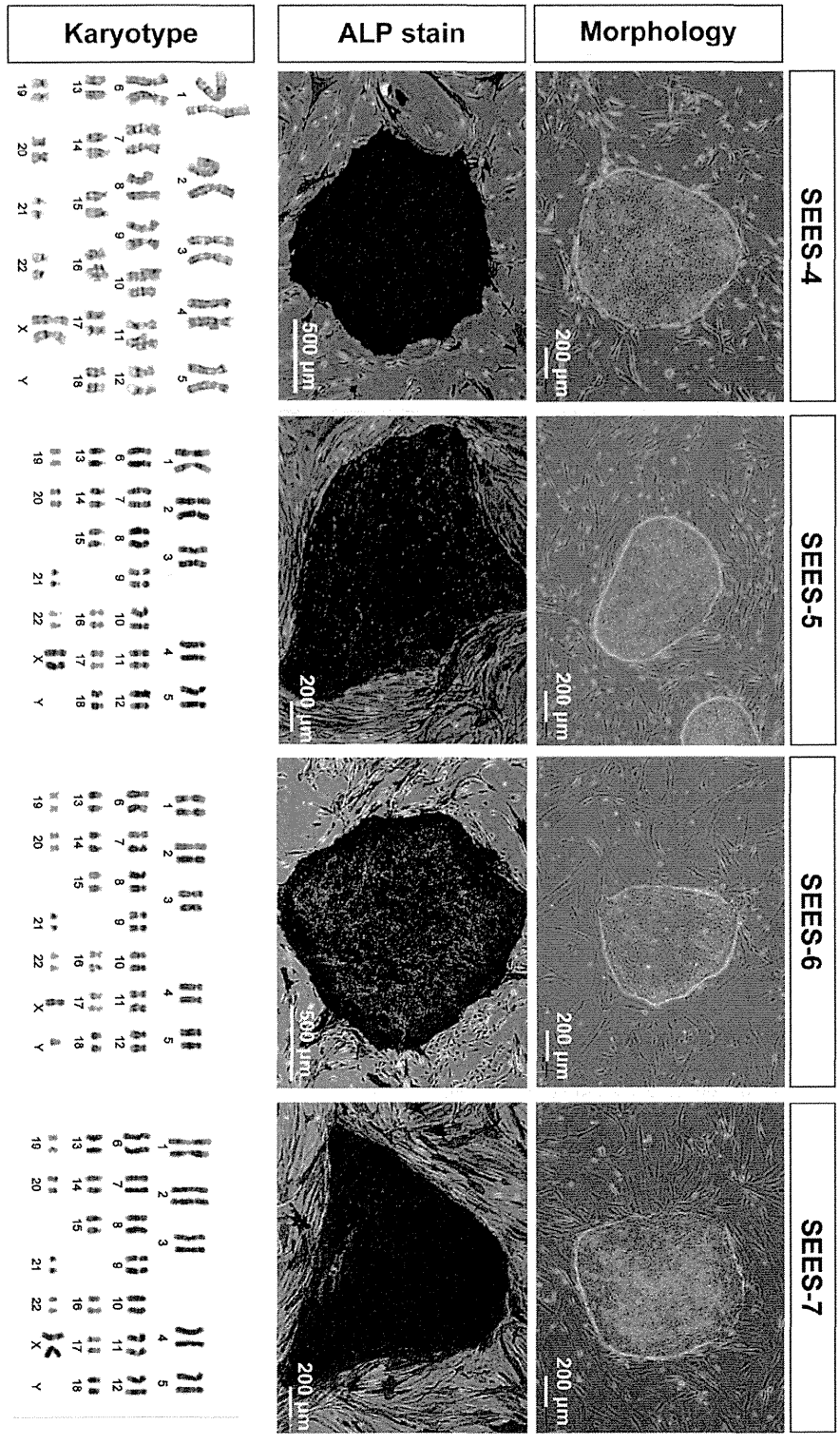

Fig. 3. Derivation of xenogeneic-free hESCs on the hMSC feeder layer Under completely xenogeneic-free conditions, four hESC lines were derived from the inactivated hMSC feeder layer using the laser ablation system. Typical ESC morphology was readily visible. Alkaline phosphatase (ALP) activity was detected in each SEES cell line. Chromosome analysis of SEES-4, SEES-5, SEES-6, and SEES-7 cells showed normal karyotypes: 46,XX, 46,XX, 46,XY, and 46,XX, respectively.

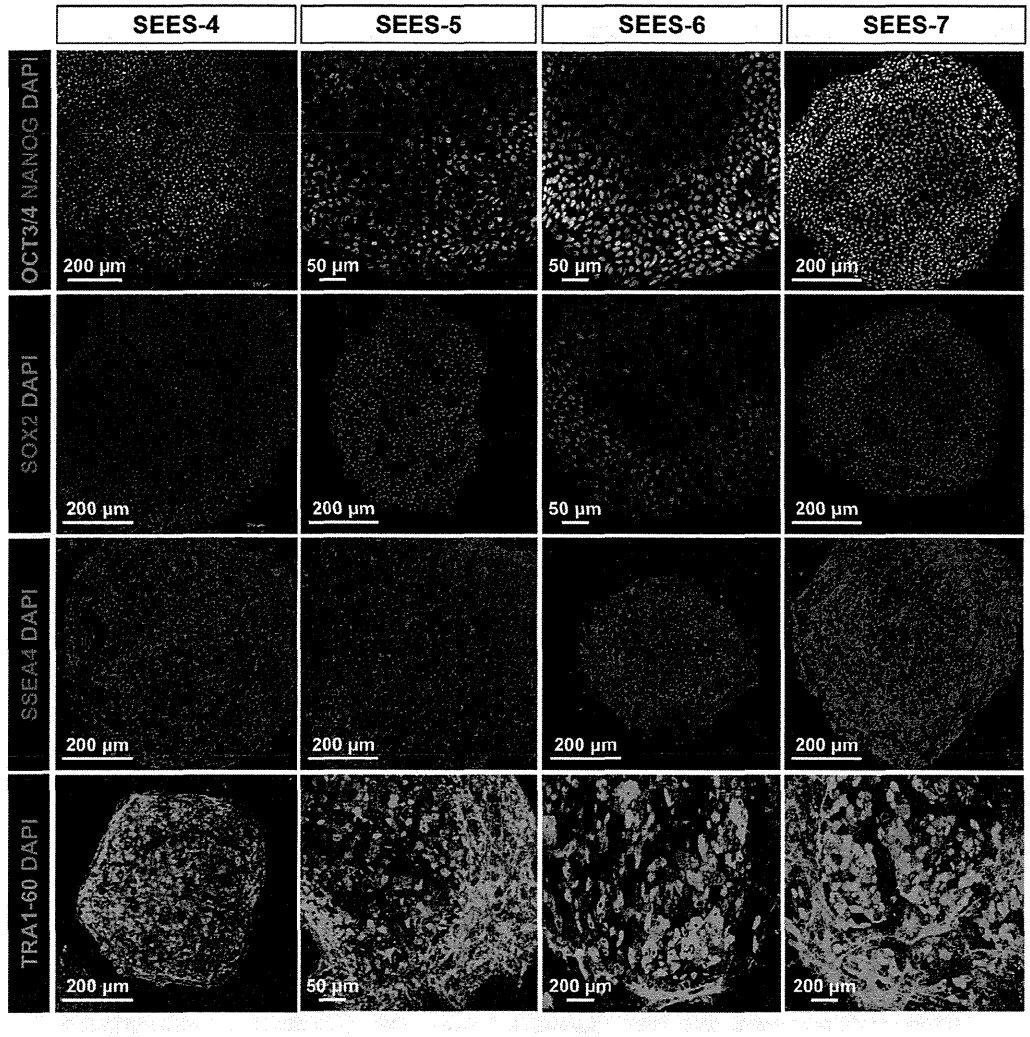

Fig. 4. Pluripotent marker expression of xenogeneic-free SEES cell lines In the undifferentiated state, xenogeneic-free SEES cell lines expressed markers characteristic of pluripotent hESCs, including OCT4, NANOG, SOX2, SSEA4, and TRA1-60. SEES-4: scale bars are 200 μm; SEES-5: scale bars are 50 μm in OCT3/4 and TRA1-60 and 200 μm in SOX2 and SSEA4; SEES-6: scale bars are 50 μm in OCT3/4 and SOX2 and 200 μm in SSEA4; SEES-7: scale bars are 200 μm.

2.5. Stable expansion of SEES cell lines under modified conventional hESC culture conditions

To overcome the shortcomings of conventional approaches, we determined which elements of conventional culture systems were necessary and sufficient for maintaining the pluripotency of hESCs. In our modified conventional hESC culture medium, human recombinant bFGF and KO-SR were replaced by pharmaceutical-grade recombinant human bFGF (trafermin) and high-dose gamma-irradiated KO-SR, respectively. SEES-2 cells were stably maintained on the qualified MEF layer in the modified medium without antibiotics (Fig. 6A). Under these conditions, the colonies expressed multiple pluripotency markers, including OCT3/4, NANOG, SOX2, SSEA4, and TRA1-60, as demonstrated by immunostaining (Fig. 6B). Interestingly, SEES-2 cells could differentiate into derivatives of all three embryonic germ layers *in vitro* and *in vivo*. The EB formation assay showed detection of TUJ1, αSMA, and AFP by immunostaining (Fig. 6C). Additionally, differentiation of the three germ layer *in vivo* was confirmed by teratoma analysis (Fig. 6D), and SEES-2 cells retained normal karyotypes following extensive passaging in culture (Fig. 6E). Under these conditions, cells were able to maintain pluripotency for over 20 passages, as confirmed by positive expression of SSEA4, TRA1-60, and TRA1-80 and absence of SSEA1 expression (Fig. 7). Taken together, our data demonstrated that the modified conventional hESC culture system, based on replacement with high-dose gamma-irradiated KO-SR and trafermin, maintained the pluripotency of hESCs. SEES-1 and SEES-3 also retaining their pluripotency, as shown by morphological analysis and immunostaining (Supplemental Fig. 7). Analysis of the expression of several genes by qRT-PCR showed that hESCs grown under conventional conditions and our modified conditions exhibited highly similar gene expression patterns (Supplemental Fig. 8). Additionally, FISH analysis of SEES cell lines showed that three out of the five SEES cell lines were X-chromosome active.

3. Discussion

Traditional methods for isolating and expanding hESCs include using MEFs as a feeder layer and supplementing medium with FBS replacement. Conventional hESC culture systems are widely used for both basic research and clinical trials under appropriate conditions for ensuring safety [15]. Currently, there are at least two options for further development of hESC cultivation systems for use in regenerative medicine; these methods seek to achieve safe

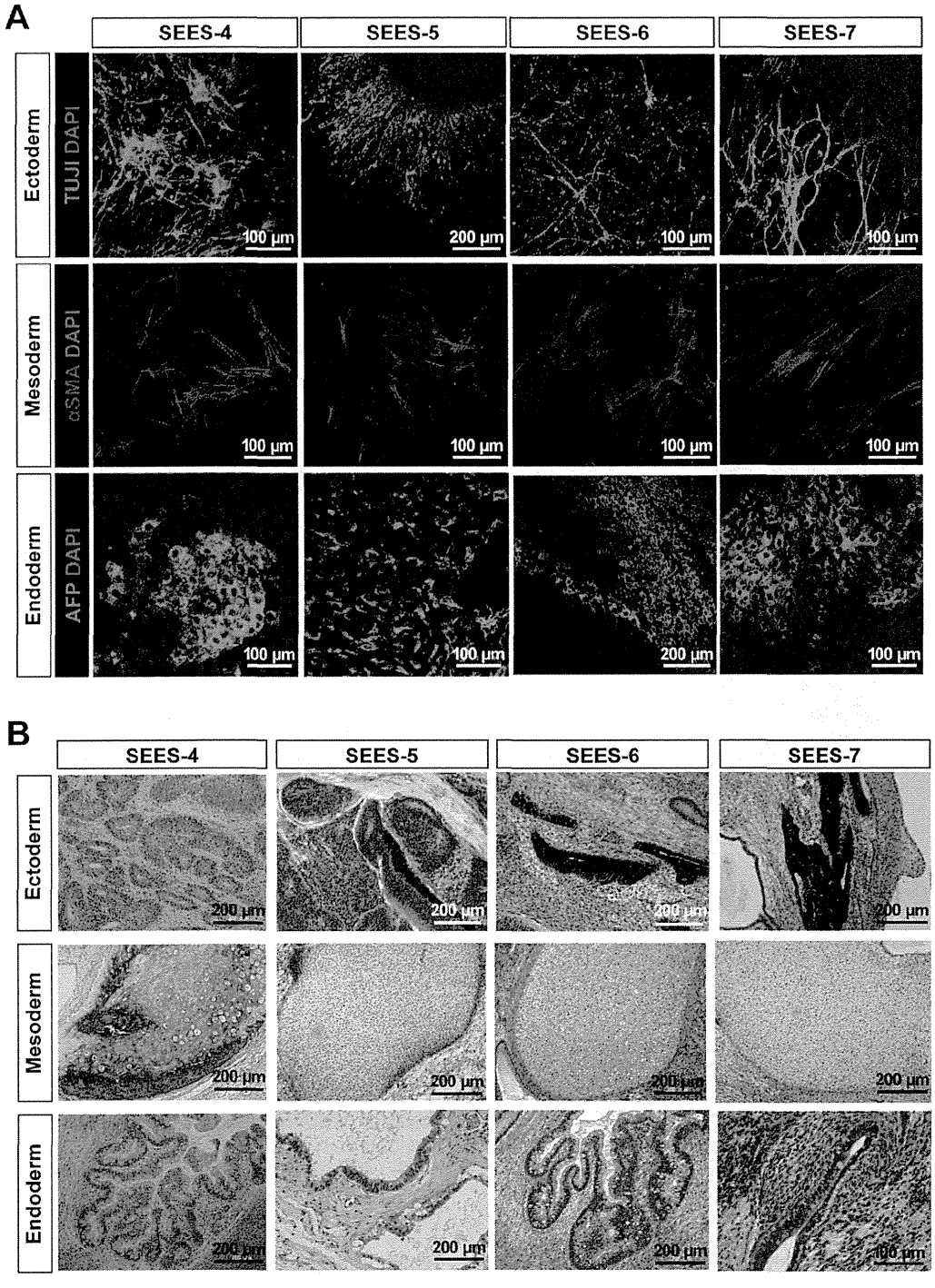

Fig. 5. Differentiation of three germ layers of xenogeneic-free SEES cell lines A) SEES cells differentiated *in vitro* via EBs expressed markers of the primary germ layers. Immunohistochemical analyses of markers of the ectoderm (TUJ1), mesoderm (αSMA), and endoderm (AFP) layers are shown. SEES-4: scale bars are 100 μm; SEES-5: scale bars are 200 μm for TUJ1 and 100 μm for αSMA and AFP; SEES-6: scale bars are 100 μm for TUJ1 and αSMA and 200 μm for AFP; SEES-7: scale bars are 100 μm. B) SEES cells differentiated *in vivo* via teratoma formation. Hematoxylin and eosin staining revealed germ layer derivatives, such as neural tissues, pigmented epithelium (ectoderm), cartilage (mesoderm), and gut epithelial tissues (endoderm). Scale bars are 200 μm.

culture conditions within a stable, conventional hESC cultivation system. Future potential uses of hESCs in clinical and industrial applications will require a reproducible, XF culture system. In this study, we evaluated the replacement of a conventional hESC culture system with high-dose, gamma-irradiated serum and pharmaceutical-grade recombinant bFGF (trafermin) in order to address the reproducibility of hESC cultivation systems. hESCs could be successfully maintained using modified conventional medium supplemented with 35 KGy-irradiated KO-SR and trafermin. Our data provided evidence supporting clinically relevant

alternative platforms of hESC culture for use in clinical and industrial applications. This study also demonstrated the development of a defined, novel, efficient culture system for the derivation of hESCs from blastocyst ICMs and described the expansion and maintenance of hESCs in completely XF conditions on human allogeneic MSC feeder layers. The XF culture system with XF hMSC feeder layers can stably expand several hiPSC lines (data not shown) and successfully allow the derivation of human iPSCs

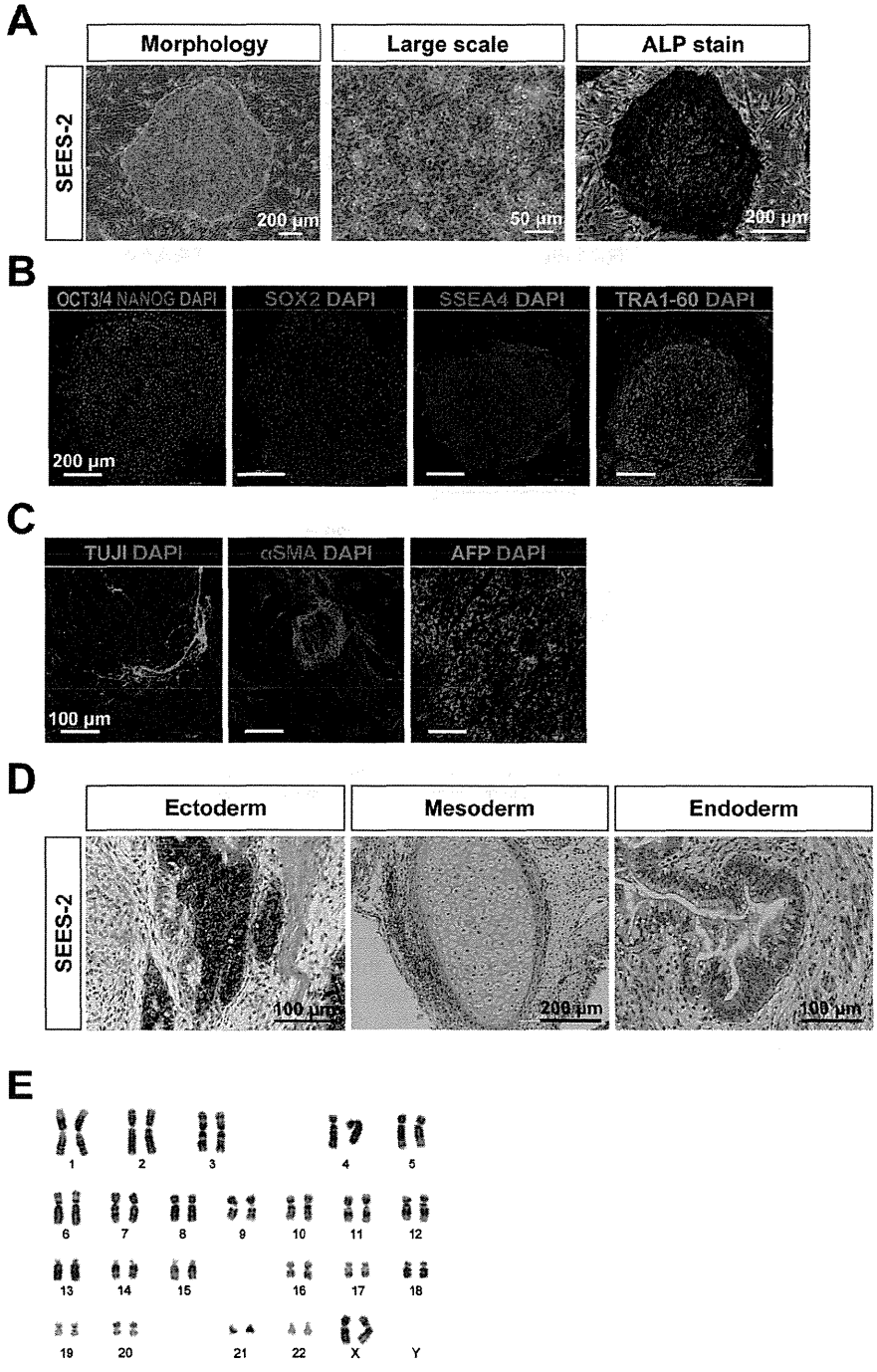

Fig. 6. Characterization of the pluripotency of SEES-2 maintained using a modified conventional hESC culture medium SEES-2 cells were stably maintained over 20 passages on the qualified MEF feeder layer in the modified medium, which contained pharmaceutical-grade recombinant human bFGF (trafermin) and high-dose (35-K) gamma-irradiated KO-SR without antibiotics. A) Typical hESC colony morphology was readily visible. ALP activity was detected. B) SEES-2 cells expressed undifferentiated hESC markers, including OCT4, NANOG, SOX2, SSEA4, and TRA1-60. SEES-2 cells could differentiate into three embryonic germ layers *in vitro* and *in vivo*. Scale bars are 200 μm. C) SEES cells that had been differentiated *in vitro* via EBs expressed markers of the primary germ layers, ectoderm (TUJ1), mesoderm (αSMA), and endoderm (AFP). Scale bars are 100 μm. D) Histological analysis of teratomas containing multidifferentiated tissues derived from SEES-2 cells. Pigmented epithelium (ectoderm), cartilage (mesoderm), and gut epithelial tissues (endoderm). E) Chromosomal analysis of SEES-2 cells cultivated through 16 passages using a modified conventional hESC culture medium showed a normal 46,XX karyotype.

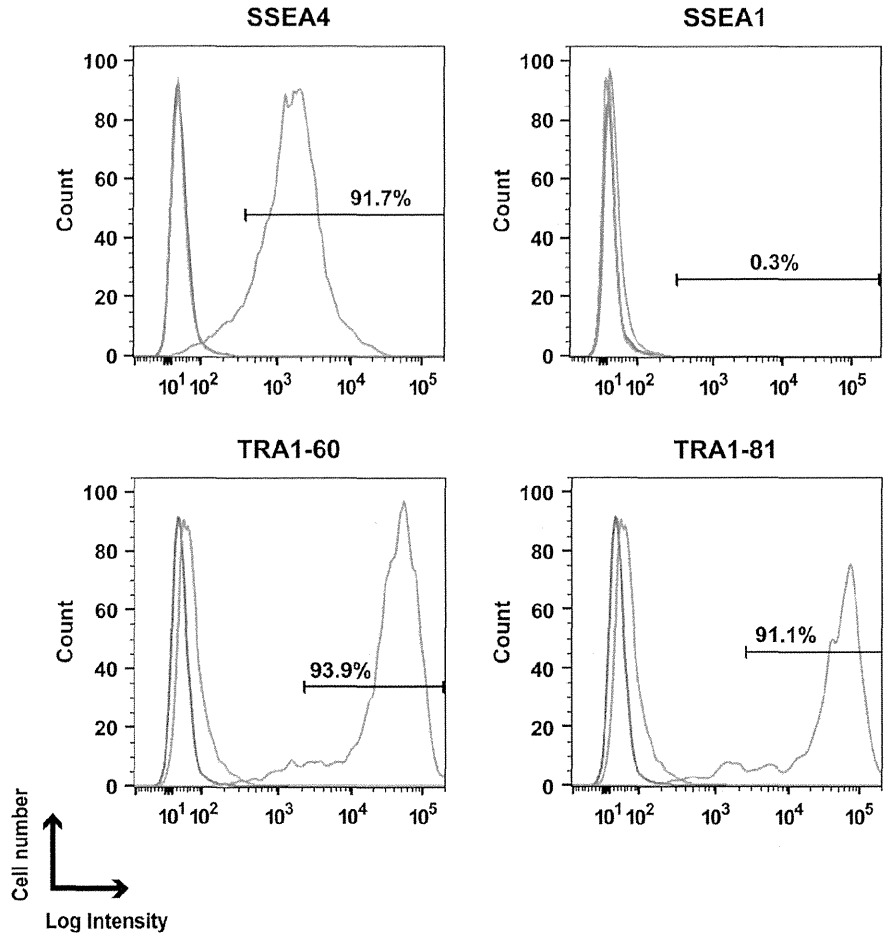

Fig. 7. Expression of pluripotency markers in SEES-2 cells was maintained using a modified conventional hESC culture medium Flow cytometric analysis of hESC-specific marker expression in SEES-2 cells. The isotype control is indicated by the blue line, and the unlabeled sample, which was used as a control, is indicated by the red line. Surface staining is shown by the yellow line for SSEA4, SSEA1, TRA-1-60, and TRA-1-81.

(Supplemental Fig. 3). These conditions are also quite applicable to iPSC derivation and cultivation as well. Importantly, the development of such an XF culture system primarily enables hESCs to culture and expand in conditions that are totally devoid of forming Neu5GC, a sialic acid glycan and xenogeneic antigen that can potentially transform cells to obtain cancer phenotypes [18,19]. In this culture system, we developed and successfully generated completely Neu5GC-free hESC lines. Our four XF hESC lines (SEES-4, SEES-5, SEES-6, and SEES-7) can be also stably cultivated under alternative xenogeneic-free conditions. Nakagawa et al. reported a novel culture system for derivation and expansion of hiPSCs with the recombinant laminin-511 E8 fragment matrices and the xenogeneic-free culture medium (StemFit™) [20]. Four XF SEES cell lines were stably grown using the StemFit™ medium under feeder-free conditions (data not shown). The XF SEES cell lines would be accustomed to being maintained in xenogeneic-free conditions with ease, as these cell lines have been derived and expanded under animal derived components-free conditions.

Pluripotent hESCs are isolated from preimplantation embryos [1] and general characteristics of hESCs include flat morphology, dependence on FGF2 signaling, differentiation into three germ layers *in vitro* and *in vivo*, and pluripotent markers expression [21]. Numerous hESC lines have been derived [3]. It is indicated that many of hESC lines differ in the manner in which they were derived and maintained in culture, and such differences may have significant effects on the characteristics of the cell lines [22,23]. In female hESCs, culture conditions may have significant effects on the X chromosome inactivation status and contribute to the cellular characteristics [24]. Three of five female SEES cell lines showed none of XIST expression in this study. However, it has demonstrated that there are not notable differences in gross hESCs characters including pluripotent markers and differentiation *in vitro* and *in vivo*, despite the significant differences in XIST expression status among SEES 1, 2, 4, 5 and 7. Notably, SEES cell lines are characterized not only the biological properties of human ESCs, also the genomic signatures including ABO blood typing, STR genotyping and HLA isotyping. The distinct properties of the SEES cell lines offer a scalable cell resource for clinical application.

The culture medium we described in this study consisted of a basal culture medium with well-known growth factors that define the maintenance of pluripotency. Since these ingredients are well known and are added to a simple culture medium formulation, the cells derived/expanded in such a system have the potential for reduced contamination, better kinetics of growth, good ability to differentiate into all the three germ layer derivative lineages, maintain a normal karyotype, and, most importantly, will not contribute to tumorigenicity. This defined culture system serves as a better and safer alternative to derive/culture/expand hESCs/iPSCs for larger cell therapy purposes.

4. Materials and methods

4.1. Derivation of hESC lines on inactivated mouse embryonic fibroblast (MEF) feeder cultures

All derivations and cultures of hESC lines in this study were performed in full compliance with the Guidelines on the Derivation and Distribution of Human Embryonic Stem Cells of the Ministry of Education, Culture, Sports, Science and Technology, Japan (Notification No. 156 of 2009), after approval of the Institutional Review Board regarding hESC research at the National Center for Child Health and Development (NCCHD; "Sei-iku" in Japanese title of the affiliation), Japan. Surplus frozen human embryos, donated by consenting couples, were thawed using a Cryotop Safety Thawing Kit (Kitazato BioPharma, Shizuoka, Japan; #VT602) according to the manufacturer's instructions and cultured in BlastAssist System medium (MediCult, Jyllinge, Denmark; #12150010) until they reached the blastocyst stage. The derivation of three hESC lines, i.e., SEES-1, SEES-2, and SEES-3, was performed using modified HUES derivation methods, as described previously [4,5,25]. Briefly, the inner cell mass (ICM) was isolated by immunosurgery by using rabbit antiserum (Rockland Immunochemicals, PA, USA; #109-4139) and guinea pig serum complement (Sigma–Aldrich, MO, USA; #S-1639) and then seeded onto a feeder layer of freshly plated gamma-irradiated MEFs, isolated from ICR embryos at 12.5 gestations and passaged two times before gamma irradiation (30 Gy), in hESC conventional derivation media. The hESC conventional derivation media consisted of Knockout Dulbecco's modified Eagle's medium (KO-DMEM; Life Technologies, CA, USA; #10829-018) supplemented with 20% Knockout Serum Replacement (KO-SR; #10828-028), 2 mM GlutaMAX-I (#35050-079), 0.1 mM nonessential amino acids (NEAAs; #11140-076), 50 U/mL penicillin/50 μg/mL streptomycin (Pen-Strep; #15070-063), 0.055 mM beta-mercaptoethanol (#21985-023), and recombinant human full-length bFGF (#PHG0261) at 10 ng/mL (all reagents were from Life Technologies). Seven to 14 days after ICMs were plated, expanded ICMs were dissected mechanically into small clumps using a finely drawn glass Pasteur pipette and transferred onto a new MEF feeder layer as previously described [4,25]. Secondary colonies were similarly dispersed and plated onto new feeder layers of MEFs until passages 2–4. Cells were then further expanded manually using a Stem Cell Cutting Tool (Vitrolife, Kungsbacka, Sweden; #14601) and Dispase II (Eidia, Ibaraki, Japan; #GD81070).

4.2. hMSCs as feeder layers

4.2.1. Production and culture of hMSCs under XF conditions

To derive and expand hMSC feeder layers under XF conditions, we eliminated the use of media with all animal-derived components during the derivation, propagation, and passaging process in the preparation of new hMSC feeders from human subjects. Parental written informed consent was obtained from all families, and the study was approved by the Institutional Review Board (IRB #88) of the NCCHD. hMSCs were isolated from human dermal tissue samples collected from juvenile donors undergoing surgical procedures for polydactyly in the Division of Orthopedics of the NCCHD. Human dermal tissues were first washed in Dulbecco's phosphate-buffered saline (DPBS) without calcium and magnesium (#14190-250) containing penicillin/streptomycin and then minced into small pieces by using a sterile scalpel in a laminar flow cabinet. The minced tissue was centrifuged and filtered in sequential steps to separate the tissue debris. The isolated cells were then expanded in StemPro MSC SFM XenoFree (MSC-XF; #A10675-01) supplemented with StemPro LipoMax Defined XenoFree Lipid Supplement (#A10850-01) on culture dishes coated with a recombinant humanized matrix (CELLstart CTS; #A10142-01). The isolated cells were expanded in MSC-XF medium with CELLstart using animal-component free TrypLE Select (#12563-011; all reagents from Life Technologies). After approximately 20 days, a confluent monolayer of primary cells was established (passage 0).

4.2.2. Proliferation assay

To assess the proliferative capacity of the isolated cells, primary cultures from two donors were analyzed through 22 serial passages using MSC-XF medium with CELLstart. Cells were counted using a cell viability analyzer (Vi-CELL Cell Viability Analyzer; Beckman Coulter, CA, USA), and cells were subcultured at 10^5 cells/100-mm dish every 4 days for approximately 15 days. At each passage, the population doubling (PD) rate was calculated based on the total cell number using the following formula: $[\log_{10}(N_h) - \log_{10}(N_1)]/\log_{10}(2)$, where N_1 was the number of cells plated and N_h was the number of cells harvested [26]. Growth curves were generated in triplicate using two independent cell lines.

4.2.3. Flow cytometric analysis and in vitro multilineage differentiation assay

Flow cytometric analysis was performed as described previously [27] in order to characterize the cells. Cells were incubated with primary antibodies or isotype-matched control antibodies, followed by immunofluorescence secondary antibody staining and analysis using an EPICS ALTRA analyzer (Beckman Coulter). The following cell surface epitopes were detected with anti-human fluorescein isothiocyanate (FITC)-conjugated or phycoerythrin (PE)-conjugated antibodies: CD29 (Beckman Coulter; #6604105), CD44 (Beckman Coulter; #IM1219), CD90 (BD Pharmingen, CA, USA; #555596), CD117 (Beckman Coulter; #IM1360), and CD133 (Miltenyi Biotec, Bergisch Gladbach, Germany; #130-080-801). The potential of the isolated cells to differentiate into osteogenic and adipogenic lineages was examined according to the manufacturer's instructions. Adipogenesis and osteogenesis were induced by culturing cells in medium from an hMSC Adipogenic BulletKit (Lonza, PA, USA; #PT-3004) or an hMSC Osteogenic BulletKit (Lonza; #PT-3002), respectively. After 8 weeks under differentiation conditions, cells were processed for lineage-specific staining. Oil red staining was used for the detection of accumulated oil droplets in the cytoplasm of cells maintained with adipogenic differentiation media. Alkaline phosphatase activity was used to determine the extent of osteogenesis in cells grown in osteogenic differentiation medium.

4.2.4. Preparation of hMSCs for the feeder layer

At passages 5–20, XF cells were detached from the culture plate with TrypLE Select, washed with MSC-XF medium, and counted. The cells were resuspended in culture medium at a concentration of 1×10^7 cells per tube and then gamma-irradiated with 30 Gy. The irradiated cells were washed in medium and frozen at a concentration of 2×10^6 cells per vial in freezing medium (STEM-CELLBANKER, ZENOAQ, Fukushima, Japan; #CB043).

4.3. XF hESCs

4.3.1. Derivation and expansion of new hESC lines under XF conditions

The procedure for derivation of XF hESCs was approved by the Institutional Review Board at the NCCHD, and embryos were collected from donors undergoing fertility treatment after obtaining informed consent. Frozen embryos were thawed and cultured to the blastocyst stage under the same methods as used for conventional hESC derivation. Blastocysts without immunosurgery were plated on inactivated XF hMSC feeder layers (Yub-1896 cells)

in XF hESC culture medium composed of 15% Knockout SR Xeno-Free CTS (KO-SR XF; Life Technologies; #12618-013), 85% KO-DMED, 2 mM GlutaMAX-I, 0.1 mM NEAAs, penicillin/streptomycin, 50 μg/mL L-ascorbic acid 2-phosphate (Sigma–Aldrich; #A4544), 10 ng/mL heregulin-1β, recombinant human NRG-beta 1/HRG-beta 1 EGF domain (R&D Systems, MN, USA; #396-HB-050/CF), 200 ng/mL LONG R^3-IGF1, recombinant human insulin-like growth factor-1 (Sigma–Aldrich; #85580C), and recombinant human full-length bFGF (Life Technologies; #PHG0261) at 20 ng/mL. Cells were initially maintained in a drawer-type incubator (IVF CUBE, ASTEC, Fukuoka, Japan; #AR-3100) at 37 °C under the appropriate humidified gas mixture (usually 3%–5% O_2/5% CO_2/90%–92% N_2). Within 7 days after whole blastocysts were plated on the feeder layers, ICMs were isolated by laser-mediated ablation of trophectoderm (TE) cells by using a XYClone laser system (Hamilton Thorne Biosciences, MA, USA) with 80% pulse strength and a pulse length of 300 μs [5]. After 2 weeks, the ICM outgrowth began to resemble morphologically distinct hESCs, and cells could be handpicked and transferred to fresh plates. After the first splitting, new colonies were disaggregated with a recombinant trypsin (Roche Applied Science, Basel, Switzerland; #06369880103) and transferred to fresh mitotically inactivated XF hMSC feeder plates every 5–7 days. Undifferentiated cells, as judged by morphology, were chosen for each further passage. A total of four XF hESC lines were derived and stably maintained (SEES-4, SEES-5, SEES-6, and SEES-7). All four SEES cell lines were maintained in a standard tissue culture incubator at 37 °C under the appropriate humidified gas mixture (3%–5% O_2/5% CO_2/90%–92% N_2) in multigas incubator (Sanyo, Osaka, Japan; #MCO-18M) in a separate culture room to avoid any contamination. SEES cells were cryopreserved using a conventional slow-rate cooling/thawing method with STEM-CELLBANKER. Validation of the cryopreservation by subsequent thawing of individual tubes resulted in efficient recovery of viable, undifferentiated hESCs.

4.3.2. Immunohistochemical analyses of stem cell and differentiated markers

Immunohistochemistry was performed as previously described [28,29]. The primary antibodies used for hESCs were specific for Nanog (1:300; ReproCELL, Kanagawa, Japan; #RCAB0003P), Oct3/4 (1:300; Santa Cruz Biotechnology, CA, USA; #sc-5279), Sox2 (1:300; Merck Millipore, Darmstadt, Germany; #AB5603), TRA1-60 (1:300; Merck Millipore; #MAB4360), and SSEA4 (1:300; Merck Millipore; #MAB4304). To assess the differentiation of the three germ layers, the primary antibodies used for embryoid bodies (EBs) were anti-α-fetoprotein (AFP; 1:200; R&D Systems; MAB1368), mouse (ascites) anti-β-tubulin III (TUJ1; 1:1000; Promega; #G712A), and anti-α-smooth muscle actin (αSMA; 1:400; Sigma; #A2547). Cells were fixed in 4% paraformaldehyde and incubated with primary antibodies overnight at 4 °C. Cells were then probed with Alexa Fluor 546 Goat Anti-Mouse IgG- or Alexa Fluor 488 Goat Anti-Rabbit IgG-conjugated secondary antibodies (1:300 each; Life Technologies), counterstained with 1 μg/mL DAPI, for 1 h in the dark at room temperature. After incubation, cells were mounted in Vectashield mounting medium containing 4′, 6-diamidino-2-phenylindole (Vector Laboratories, CA, USA). The labeled cells were visualized using a laser-scanning confocal microscope (LSM 510 META; Carl Zeiss, Oberkochen, Germany). Alkaline phosphatase (ALP) was detected with a Vector Red kit (Vector Laboratories; #SK-5100) according to manufacturer's instructions.

4.3.3. Flow cytometry analysis of pluripotency markers

SEES cells cultured in appropriate conditions were stained for 30 min at 4 °C with primary antibodies and immunofluorescence secondary antibodies. Cells were analyzed with a Cytomics FC 500 Cytometer (Beckman Coulter), and data were analyzed with FC 500 CXP Software ver. 2.0 (Beckman Coulter). Antibodies against human SSEA-1 (R&D Systems; #FAB2155C), SSEA4 (R&D Systems; #FAB1435F), TRA1-60 (Merck Millipore; #MAB4360), and TRA1-81 (Merck Millipore; #MAB4381) were used as primary antibodies in hESCs. PE-conjugated anti-mouse IgG antibodies (BD Pharmingen; #555578) and PE-conjugated anti-mouse IgM antibodies (BD Pharmingen; #553472) were used as secondary antibodies. X-Mean, the sum of intensity divided by the total cell number, was automatically calculated and was utilized for our evaluation.

4.3.4. Differentiation assays in vitro and in vivo

For induction of differentiation *in vitro*, the cells were dissociated using either StemPro Accutase (Life Technologies; #A11105-01) or TrypLE Select for 5 min at 37 °C, plated into 96-well plates (low attachment surface; Lipidure; NOF Corp., Tokyo, Japan), and cultured in differentiation medium containing KO-DMEM supplemented with 20% fetal bovine serum (FBS), 2 mM GlutaMAX-I, 0.1 mM NEAAs, and penicillin/streptomycin, to generate EBs. After 7 days in suspension, EBs were transferred onto poly-L-ornithine-coated chamber slides and cultured for an additional 10–14 days. The cultures were fixed with 4% paraformaldehyde for 20 min before immunohistochemical analysis.

In vivo pluripotency was assessed by teratoma formation in severe combined immunodeficient nude mice (BALB/cAJcl-nu/nu) purchased from CLEA Japan. A 60-mm plate of undifferentiated hESCs was washed with DPBS, and the cells were harvested with a cell scraper. The cell suspension was collected into a 15-mL conical tube and centrifuged at 1000 rpm for 4 min. The cell pellet was resuspended in hESC culture medium and Matrigel (BD Biosciences, NJ, USA; #356234) to a final total volume of 400 μL. Approximately $2–5 \times 10^6$ cells in 200 μL were injected subcutaneously into the dorsolateral area on both sides. Mice were sacrificed after 8–10 weeks. Tumors were then excised surgically, fixed in 4% paraformaldehyde, embedded in paraffin, sectioned, and stained with hematoxylin and eosin. Hematoxylin and eosin-stained paraffin-embedded sections were histologically examined for the presence of differentiated human tissue derived from all three embryonic germ layers.

The animal use protocol was approved by the Institutional Animal Care and Use Committee of the National Research Institute for Child Health and Development (NRICHD, Permit Number: A2003-002). All experiments with mice were subject to the 3 R consideration (refine, reduce, and replace), and all efforts were made to minimize animal suffering and to reduce the number of animals used.

4.3.5. Sialic acid analysis

Sialic acid was released from cell homogenate samples by acid hydrolysis with 0.05 M HCl at 80 °C for 3 h. Sialic acid samples were ultrafiltered using Amicon Ultra-0.5 mL filters (cut-off, 10 kDa; Millipore; #UFC503008), and filtrates were dried in a vacuum concentrator. Sialic acid was derivatized with 1,2-diamino-4,5-methylenedioxybenzene (DMB; Sialic Acid Fluorescence Labeling Kit; Takara Bio, Shiga, Japan) and analyzed by reverse-phase fluorometric HPLC1 using a PALPAK Type R column (Takara Bio). The excitation and emission wavelengths were 310 and 448 nm, respectively. The DMB-derivatized sialic acid was identified by comparing retention times with those of known standards (Glyko Sialic acid reference panel; ProZyme, CA, USA; #GKRP-2503) that were similarly treated. This method can evaluate sialic acids at a minimum concentration of 0.01 nmol/mg protein.

4.3.6. Karyotype analysis

Chromosomal G-band analyses were performed at the Nihon Gene Research Laboratories, Sendai, Japan. The chromosomes were

classified according to the International System for Human Cytogenetic Nomenclature. At least 20 metaphase chromosomes were analyzed per cell line.

4.4. Generation of human iPSCs

Human iPSCs were generated from XF Yub-1896 cells by transduction with of a lentiviral vector carrying three reprogramming factors (OCT3/4, SOX2 and KLF4) under XF culture conditions. The vector was a generous gift of Konrad Hochedlinger (Harvard University). XF iPSCs were successfully maintained on inactivated XF hMSC feeder layers in XF hESC culture medium over 20 passages. We confirmed the XF iPSCs expressed pluripotent markers including OCT3/4, NANOG, SSEA4, and TRA1-60.

4.5. Modified conventional hESC cultivation

4.5.1. Production of MEF feeder stock

Pregnant ICR mice were obtained from a breeding colony under specific pathogen-free (SPF) conditions in a barrier room with extensive health monitoring at CLEA Japan (Atsugi facility, Kanagawa, Japan). MEFs were generated from ICR embryos at 12.5 gestations as previously described [5,25] and expanded using MEF feeder sock medium composed of 90% KO-DMEM, 30 KGy gamma-irradiated FBS (HyClone; Thermo Fisher Scientific, MA, USA), and 2 mM GlutaMAX-I without any antibiotics. At passage 2, cells were mitotically inactivated by gamma irradiation (30 Gy) and frozen at a concentration of 4×10^6 cells per vial. To minimize the risk of introducing murine viruses and other pathogens, MEF feeder stock was tested in GMP/GLP studies by Vitology Limited (Glasgow, UK). The specifications and results for the testing of lot MEF-0001 are presented in Supplemental Table 3.

4.5.2. hESC expansion using gamma-irradiated KO-SR and pharmaceutical-grade recombinant human bFGF without antibiotics

To develop a safer culture system for clinical application of hESCs, we replaced KO-SR and recombinant human full-length bFGF with pharmaceutical recombinant human bFGF and high-dose gamma–irradiated KO-SR. Frozen KO-SR products ware gamma irradiated at 35 KGy (KOGA ISOTOPE, Ltd., Shiga, Japan). Pharmaceutical-grade recombinant human bFGF (generic name: trafermin), supplied by Kaken Pharmaceutical (Tokyo, Japan) as Fiblast Spray, which is prepared using the powdered form of trafermin, was applied for hESC culture. hESC lines were cultivated in a modified conventional culture medium composed of 20% gamma-irradiated KO-SR, 80% KO-DMEM, 2 mM GlutaMAX-I, 0.1 mM NEAAs, and 50 ng/mL trafermin without any antibiotics on plates coated with 0.1% type I collagen (Nippon Ham, Ibaraki, Japan; #307-31611) and a mitotically inactivated layer of MEFs.

Competing financial interests

The authors declare no competing financial interests.

Acknowledgments

We are grateful to Hideki Tsumura and the staff of the Animal Care Facility at NRICHD for mouse husbandry. We thank Kaken Pharmaceutical for providing us with the trafermin used in this study. We thank Kahori Minami and Nobuyuki Watanabe for technical assistance and Tomoyuki Kawasaki for help with editing the figures. The authors would like to thank members of the Umezawa laboratory for helpful suggestions.

This research was supported by grants from the Ministry of Education, Culture, Sports, Science, and Technology (MEXT) of Japan; by Ministry of Health, Labor and Welfare (MHLW) Sciences research grants; by a Research Grant on Health Science focusing on Drug Innovation from the Japan Health Science Foundation; by the program for the promotion of Fundamental Studies in Health Science of the Pharmaceuticals and Medical Devices Agency; by the Grant of National Center for Child Health and Development; by the Takeda Science Foundation to HA and AU. This research was also by a grant from JST-CREST to HA. AU acknowledges the International High Cited Research Group (IHCRG #14-104), Deanship of Scientific Research, King Saudi University, Riyadh, Kingdom of Saudi Arabia. AU also thanks King Saud University, Riyadh, Kingdom of Saudi Arabia, for the Visiting Professorship. The funders had no control over the study design, data collection and analysis, decision to publish, or preparation of the manuscript.

Appendix A. Supplementary data

Supplementary data related to this article can be found at http://dx.doi.org/10.1016/j.reth.2014.12.004.

References

[1] Thomson JA, Itskovitz-Eldor J, Shapiro SS, Waknitz MA, Swiergiel JJ, Marshall VS, et al. Embryonic stem cell lines derived from human blastocysts. Science 1998;282:1145–7.
[2] Schuldt BM, Guhr A, Lenz M, Kobold S, MacArthur BD, Schuppert A, et al. Power-laws and the use of pluripotent stem cell lines. PLoS One 2013;8:e52068.
[3] Amit M, Carpenter MK, Inokuma MS, Chiu CP, Harris CP, Waknitz MA, et al. Clonally derived human embryonic stem cell lines maintain pluripotency and proliferative potential for prolonged periods of culture. Dev Biol 2000;227:271–8.
[4] Cowan CA, Klimanskaya I, McMahon J, Atienza J, Witmyer J, Zucker JP, et al. Derivation of embryonic stem-cell lines from human blastocysts. N Engl J Med 2004;350:1353–6.
[5] Chen AE, Egli D, Niakan K, Deng J, Akutsu H, Yamaki M, et al. Optimal timing of inner cell mass isolation increases the efficiency of human embryonic stem cell derivation and allows generation of sibling cell lines. Cell Stem Cell 2009;4:103–6.
[6] Xu C, Inokuma MS, Denham J, Golds K, Kundu P, Gold JD, et al. Feeder-free growth of undifferentiated human embryonic stem cells. Nat Biotechnol 2001;19:971–4.
[7] Richards M, Fong CY, Chan WK, Wong PC, Bongso A. Human feeders support prolonged undifferentiated growth of human inner cell masses and embryonic stem cells. Nat Biotechnol 2002;20:933–6.
[8] Martin MJ, Muotri A, Gage F, Varki A. Human embryonic stem cells express an immunogenic nonhuman sialic acid. Nat Med 2005;11:228–32.
[9] Pham T, Gregg CJ, Karp F, Chow R, Padler-Karavani V, Cao H, et al. Evidence for a novel human-specific xeno-auto-antibody response against vascular endothelium. Blood 2009;114:5225–35.
[10] Varki A. Colloquium paper: uniquely human evolution of sialic acid genetics and biology. Proc Natl Acad Sci U S A 2010;107(Suppl. 2):8939–46.
[11] Ludwig TE, Levenstein ME, Jones JM, Berggren WT, Mitchen ER, Frane JL, et al. Derivation of human embryonic stem cells in defined conditions. Nat Biotechnol 2006;24:185–7.
[12] Lu J, Hou R, Booth CJ, Yang SH, Snyder M. Defined culture conditions of human embryonic stem cells. Proc Natl Acad Sci U S A 2006;103:5688–93.
[13] Yao S, Chen S, Clark J, Hao E, Beattie GM, Hayek A, et al. Long-term self-renewal and directed differentiation of human embryonic stem cells in chemically defined conditions. Proc Natl Acad Sci U S A 2006;103:6907–12.
[14] Hasegawa K, Pomeroy JE, Pera MF. Current technology for the derivation of pluripotent stem cell lines from human embryos. Cell Stem Cell 2010;6:521–31.
[15] Schwartz SD, Hubschman JP, Heilwell G, Franco-Cardenas V, Pan CK, Ostrick RM, et al. Embryonic stem cell trials for macular degeneration: a preliminary report. Lancet 2012;379:713–20.
[16] Fraga AM, Souza de Araújo E, Stabellini R, Vergani N, Pereira LV. A survey of parameters involved in the establishment of new lines of human embryonic stem cells. Stem Cell Rev 2011;7:775–81.
[17] Wang L, Schulz TC, Sherrer ES, Dauphin DS, Shin S, Nelson AM, et al. Self-renewal of human embryonic stem cells requires insulin-like growth factor-1 receptor and ERBB2 receptor signaling. Blood 2007;110:4111–9.
[18] Hedlund M, Padler-Karavani V, Varki NM, Varki A. Evidence for a human-specific mechanism for diet and antibody-mediated inflammation in carcinoma progression. Proc Natl Acad Sci U S A 2008;105:18936–41.
[19] Pearce OM, Läubli H, Verhagen A, Secrest P, Zhang J, Varki NM, et al. Inverse hormesis of cancer growth mediated by narrow ranges of tumor-directed antibodies. Proc Natl Acad Sci U S A 2014;111:5998–6003.

[20] Nakagawa M, Taniguchi Y, Senda S, Takizawa N, Ichisaka T, Asano K, et al. A novel efficient feeder-free culture system for the derivation of human induced pluripotent stem cells. Sci Rep 2014;4:3594.
[21] Hanna JH, Saha K, Jaenisch R. Pluripotency and cellular reprogramming: facts, hypotheses, unresolved issues. Cell 2010;143:508–25.
[22] Hoffman LM, Carpenter MK. Characterization and culture of human embryonic stem cells. Nat Biotechnol 2005;23:699–708.
[23] Hoffman LM, Hall L, Batten JL, Young H, Pardasani D, Baetge EE, et al. X-inactivation status varies in human embryonic stem cell lines. Stem Cells 2005;23:1468–78.
[24] Nguyen HT, Geens M, Spits C. Genetic and epigenetic instability in human pluripotent stem cells. Hum Reprod Update 2013;19:187–205.
[25] Akutsu H, Cowan CA, Melton D. Human embryonic stem cells. Methods Enzymol 2006;418:78–92.
[26] Escobedo-Lucea C, Bellver C, Gandia C, Sanz-Garcia A, Esteban FJ, Mirabet V, et al. A xenogeneic-free protocol for isolation and expansion of human adipose stem cells for clinical uses. PLoS One 2013;8:e67870.
[27] Cui CH, Miyoshi S, Tsuji H, Makino H, Kanzaki S, Kami D, et al. Dystrophin conferral using human endothelium expressing HLA-E in the non-immunosuppressive murine model of Duchenne muscular dystrophy. Hum Mol Genet 2011;20:235–44.
[28] Nagata S, Toyoda M, Yamaguchi S, Hirano K, Makino H, Nishino K, et al. Efficient reprogramming of human and mouse primary extra-embryonic cells to pluripotent stem cells. Genes Cells 2009;14:1395–404.
[29] Makino H, Toyoda M, Matsumoto K, Saito H, Nishino K, Fukawatase Y, et al. Mesenchymal to embryonic incomplete transition of human cells by chimeric OCT4/3 (POU5F1) with physiological co-activator EWS. Exp Cell Res 2009;315:2727–40.

References in supplemental figures

[1] Hosoi E. Biological and clinical aspects of ABO blood group system. J Med Invest 2008;55:174–82 (For Supplemental Figure S1).
[2] Ota M, Fukushima H, Kulski JK, Inoko H. Single nucleotide polymorphism detection by polymerase chain reaction-restriction fragment length polymorphism. Nat Protoc 2007;2:2857–64 (For Supplemental Figure S2).
[3] Muro T, Fujihara J, Imamura S, Nakamura H, Kimura-Kataoka K, Toga T, et al. Determination of ABO genotypes by real-time PCR using allele-specific primers. Leg Med Tokyo 2012;14:47–50 (For Supplemental Figure S3).